CYTOSKELETAL MOTORS

Moving into the cell: single-molecule studies of molecular motors in complex environments

Claudia Veigel[*‡] *and Christoph F. Schmidt*[§]

Abstract | Much has been learned in the past decades about molecular force generation. Single-molecule techniques, such as atomic force microscopy, single-molecule fluorescence microscopy and optical tweezers, have been key in resolving the mechanisms behind the power strokes, 'processive' steps and forces of cytoskeletal motors. However, it remains unclear how single force generators are integrated into composite mechanical machines in cells to generate complex functions such as mitosis, locomotion, intracellular transport or mechanical sensory transduction. Using dynamic single-molecule techniques to track, manipulate and probe cytoskeletal motor proteins will be crucial in providing new insights.

Molecular motors are machines that convert free energy, mostly obtained from ATP hydrolysis, into mechanical work. The cytoskeletal motor proteins of the myosin and kinesin families, which interact with actin filaments and microtubules, respectively, are the best understood. Less is known about the dynein family of cytoskeletal motors, which interact with microtubules. Cytoskeletal motors power diverse forms of motility, ranging from the movement of entire cells (as occurs in muscular contraction or cell locomotion) to intracellular structural dynamics (as occurs in membrane trafficking or mitosis) and mechanical signal transduction (as occurs in hair cells of the inner ear[1]). Such diverse functions are possible because the structure and regulation of motors in each family can vary largely, despite strong similarities in their catalytic cores.

As discussed in detail in other Reviews in this series[2–6], myosin and kinesin motors contain a catalytic domain, which includes a nucleotide-binding region and an actin- or microtubule-binding site (FIG. 1A), and this is followed by a neck region. The neck is followed by a tail domain, which often contains an α-helical section (called a stalk domain in kinesins) and ends in a cargo-binding domain. Many motors dimerize by forming helical coiled-coils through their tails or stalks. During the motor's ATPase cycle, nucleotide hydrolysis and the release of hydrolysis products at the nucleotide-binding site[7–9] are coupled to small movements within the catalytic domain, which are amplified by mechanical elements connected to the catalytic domain, specifically, the neck linker in kinesins[10] and the α-helical lever-arm in myosins[11]. Structural data suggest that during the force-generating conformational change, known as the power stroke, the lever arm of myosins[8,11] rotates around its base at the catalytic domain[11–17], which can cause the displacement of bound cargo by several nanometres[18] (FIG. 1B). In kinesins, the switching of the neck linker (~13 amino acids connecting the catalytic core to the cargo-binding stalk domain) from an 'undocked' state to a state in which it is 'docked' to the catalytic domain, is the equivalent of the myosin power stroke[10]. Neck-linker docking propels the trailing head and the cargo forward (FIG. 1C). Most molecular motors produce directional movement; that is, a given class of motors moves towards either the plus end or minus end of the polarised actin filaments or microtubules.

Complementary approaches have provided insight into the structure and function of motors. Bulk biochemical methods have revealed the kinetics of the ATPase reaction cycle[8,19,20] and X-ray crystallography has delivered atomic-scale structures of motors in different conformations, mainly using crystals of the motors' catalytic domains[8,21,22]. Less is known about the atomic structure of the neck region of myosins[23–25] and the cargo-binding tail domains of myosins and kinesins. Electron microscopy (EM) has made it possible to image single motor molecules that have been fixed or frozen in near-physiological conditions and to characterize them in full-size, multimeric or bundled states, or bound to their filament tracks. By providing snapshots of individual states, EM studies have given clues about the progression of motors through their chemomechanical cycles[10,16,26–32] and have revealed some

*Department of Cellular Physiology, Institute of Physiology, Ludwig-Maximilians-Universität München, Schillerstrasse 44, 80336 München, Germany.
‡Centre for NanoScience, Universität München, Schillerstrasse 44, 80336 München, Germany.
§Drittes Physikalisches Institut, Georg-August-Universität Göttingen, Friedrich-Hund-Platz 1, 37077 Göttingen, Germany.
e-mails: claudia.veigel@med.uni-muenchen.de; cfs@physik3.gwdg.de
doi:10.1038/nrm3062
Published online 16 February 2011

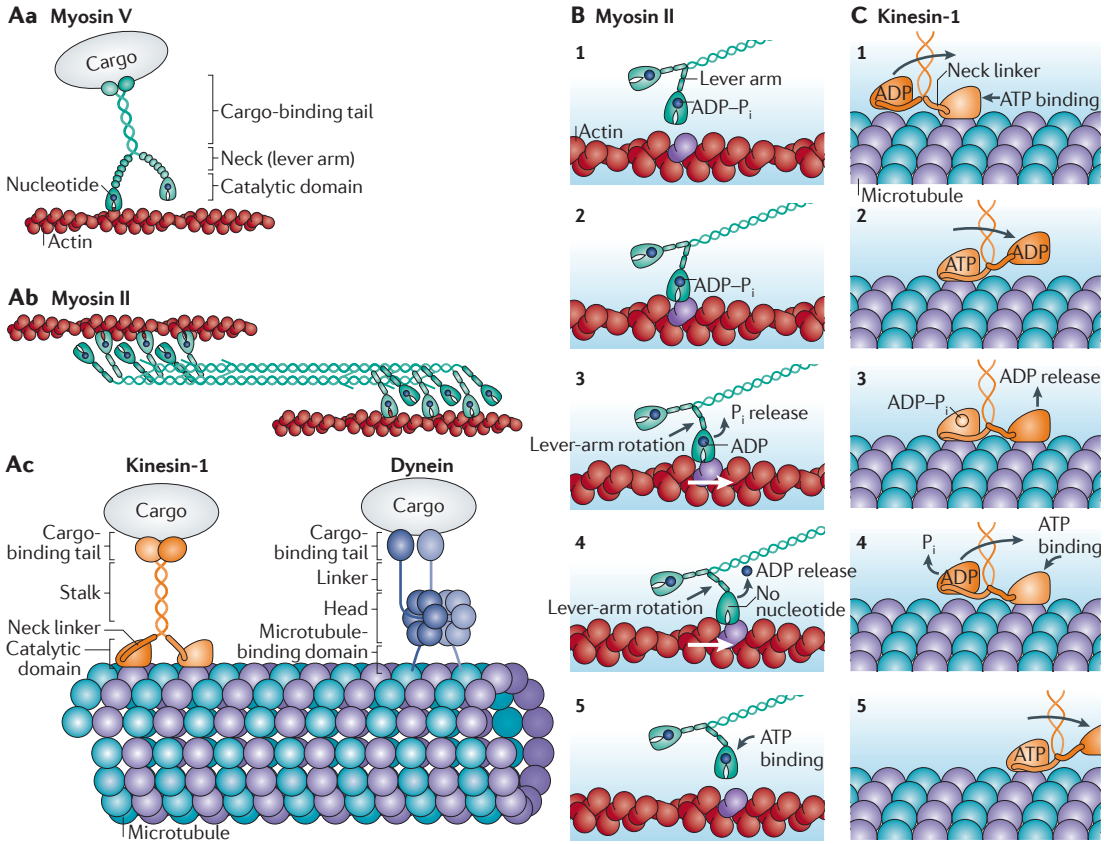

Figure 1 | **Cytoskeletal motor structures and functions. Aa** | Myosin V works as a dimer to 'processively' transport intracellular cargo along actin filaments. Its functional segments are labelled. **Ab** | 'Non-processive' dimeric myosin II has similar functional domains to myosin V but assembles in a different manner. Several proteins associate through their tail domains into bipolar filaments that can exert tension between actin filaments. **Ac** | Kinesins and dyneins move along microtubules. Kinesin-1 and cytoplasmic dynein (shown in the figure) are processive and move intracellular cargo. Kinesins have a similar domain structure to myosins (functional segments are labelled). Dynein also acts as a dimer, but it is structurally different from other cytoskeletal motors. **B** | Structural changes of a myosin II head during its power stroke. The respective nucleotide state is indicated. The motor head starts in an unbound state (step **1**), then binds to actin with the products of ATP hydrolysis, ADP and inorganic phosphate (P_i), bound to the catalytic site (step **2**). The release of P_i is coupled to a first lever-arm rotation, which causes actin to move (step **3**; actin movement is indicated by the white arrow). Release of ADP causes a second, smaller rotation of the lever arm and additional actin movement (step **4**). ATP binding induces detachment of the motor (step **5**). **C** | Structural changes of a dimeric Kinesin-1 during a processive step, with nucleotide states indicated. ATP binding to the bound head (step **1**) causes neck-linker docking, which directs the unbound head forward to the next binding site along the microtubule (step **2**). Binding at this site causes ADP release (step **3**). ATP hydrolysis followed by P_i release causes the now trailing head to detach (step **4**). ATP binding to the leading head again causes neck-linker docking, and the cycle repeats (step **5**). Figures in parts **B** and **C** are modified, with permission, from REF. 186 © (2000) AAAS.

principles of regulation; for example, by showing that the cargo-binding tails fold backwards in some myosins and kinesins, thereby inhibiting the catalytic domain[33–37]. Studies of motors harbouring a missense mutation or a large domain change, such as the addition of an artificial lever arm, have provided important insight into the function of structural parts[22]. Imaging of single actin filaments and microtubules *in situ* in cells is now within reach with high-resolution electron tomography[38]. However, EM is a static technique. The dynamics of intramolecular motion, domain folding and unfolding, and the force generation and energy conversion of motor proteins in physiological conditions, can only be investigated by dynamic single-molecule techniques.

In this Review, we focus on new developments in dynamic single-molecule techniques, specifically atomic force microscopy (AFM), single-molecule fluorescence microscopy and optical tweezers. We discuss how they can be used to study the basic mechanisms of cytoskeletal motors, both *in vitro* and in cells, and what the application of these techniques has already shown us about the mechanisms of cytoskeletal motor movement.

Why use single-molecule techniques?

About 25 years ago, the first gliding-filament assays and bead assays were introduced to study cytoskeletal motors[39–42]. In the gliding-filament assays, motors were immobilized on a microscope cover slip and video

microscopy was used to observe how these motors could move actin or microtubule filaments[42]. In bead assays, the movement of micron-sized beads by single motor proteins along immobilized filaments was monitored (as in FIG. 1A but with the cargo replaced by a bead). These assays revealed that 'non-processive' motors, such as muscle myosin II[18,43] and the Kinesin-14 Non-claret disjunctional (NCD)[44–46], perform isolated power strokes: they transiently exert force or produce motion and then unbind from their track (FIG. 1B). By contrast, the 'processive' motors, such as homodimeric Kinesin-1 (REF. 47), myosin V[48] and cytoplasmic dynein[49–51], move along their tracks for many successive chemomechanical cycles by alternatingly keeping one head bound to the track while moving forward with the other head. They can thus take tens to hundreds of steps before detaching (FIG. 1C). Many critical details of the basic mechanism of chemomechanical energy transduction and, particularly, how it is regulated by cargo, load conditions and intramolecular strain ('gating') are still not clear.

Continual technological progress made since the first single-molecule mechanical experiments were designed is described in recent reviews[52–54]. Single-molecule approaches have allowed us to determine many basic parameters of the chemomechanical energy transduction of cytoskeletal motors, including step sizes[18,43,47,55–57] and forces[48,55,57–61]. Sophisticated single-molecule experiments have shown that there is coupling between the chemical and mechanical cycles[62,63], and that the generation of force in mechanical sub-steps is tightly coupled to biochemical transitions[45,64–66] and is load dependent[67–69]. For dynein, it was shown that helix sliding is involved in allosteric signalling between catalytic sites and filament-binding sites[70]. A hand-over-hand mechanism was firmly established as the mode of locomotion of processive kinesin and myosin motors[71–74] (FIG. 1C) and, in elegant experiments in which a single kinesin head was linked to a bead by a DNA tether, the load-dependent forward-stepping of a single head could be directly observed[75]. Furthermore, it was demonstrated that processive movement[76,77], and even the force-generating power stroke itself, is reversible in direction[67]. The reversibility of the power stroke while the motor is attached to the target implies that there might be mechanical coordination or synchronization of motors in the cell under load.

The dynamic single-molecule techniques we discuss in this Review make it possible to gather complementary types of information on molecular motors. AFM can provide nanometre-resolution structural information on the domain conformations of isolated and filament-bound motors in close to physiological conditions. For AFM, the sample needs to be fixed to a surface, which precludes imaging within cells. Fluorescence and other light microscopy techniques can be used to localize single motor molecules and quantify their movement both *in vitro* and in cells. One can even measure the conformational changes of molecular sub-domains dynamically with single-nanometre spatial and millisecond temporal resolution using spectroscopic methods such as Förster resonance energy transfer (FRET). Finally, optical and magnetic tweezers can measure displacements and forces generated by single motor proteins. By characterizing the effects of load, it is possible to explore the chemomechanical 'free-energy landscape' that motors act in and to map out the activation energy barriers between different biochemical and mechanical states in the motors' cycles.

Förster resonance energy transfer
Non-radiative energy transfer from an excited donor fluorophore to an acceptor fluorophore in the immediate vicinity can be used to measure nanometre distances owing to the strong distance-dependence of the effect.

Single-molecule imaging using AFM

AFM can image moving biomolecules in buffer[78]. Positional resolution of several nanometres can be achieved, but it typically takes hundreds of milliseconds to record one image. Conformational changes of motors occur in tens of milliseconds or less and thus cannot currently be resolved with this technique. AFM can be used in force-spectroscopy mode or imaging mode. In imaging mode, a compliant mechanical lever arm (cantilever) with a sharp tip is used to sample the height profile of an immobilized structure (FIG. 2a). Biomolecules are often adsorbed electrostatically to chemically derivatized surfaces. Surfaces can be mica, silicon chips or polished glass. Cantilevers have bending elastic constants (K) of between 10 and 10,000 pN nm^{-1}. Forces on the cantilever tip are measured by its deflection. The smallest forces that can be reliably measured are tens of piconewtons. In force-spectroscopy mode, the molecule of interest is positioned with one end fixed to a surface and the other end attached to the cantilever tip, such that tension can be applied by moving the cantilever (FIG. 2b). This approach has been used extensively to study the dynamics of unfolding and refolding of a large range of proteins and other biomacromolecules[78]. The force-dependent unfolding kinetics of the kinesin neck coiled-coil (the beginning of the region linking the two heads) has been studied in this manner[79]. The neck coiled-coil is thought to be critical for mechanical communication between the heads, and high-resolution experiments showed that the neck linker forms an exceptionally stable coiled-coil, which ensures efficient force transmission between the heads.

In studies using imaging mode, the protofilament substructure of microtubules was resolved[80–82]. Truncated kinesins that were strongly bound to microtubules by the non-hydrolysable ATP analogue AMP-PNP, which stops motors on their tracks, were imaged with single-head resolution (FIG. 2c). Even moving motors could be seen transiently[83]. The first AFM recording at video frame rate (25 frames per second) of an entire, unlabelled motor protein was achieved for myosin V motor proteins moving processively along an actin filament[84,85] (FIG. 2d). With improvements in sample preparation and in the quality and control of the AFM tip, it recently became possible to resolve even the movement of individual protein sub-domains, on the timescale of ~100 ms, in experiments with single myosin V molecules moving along actin[84].

Single-molecule fluorescence microscopy

To localize and track single molecular motors and cytoskeletal filaments using fluorescence microscopy, more photons need to be collected from the motor than from the background. This is typically achieved by restricting the sample volume and by working at

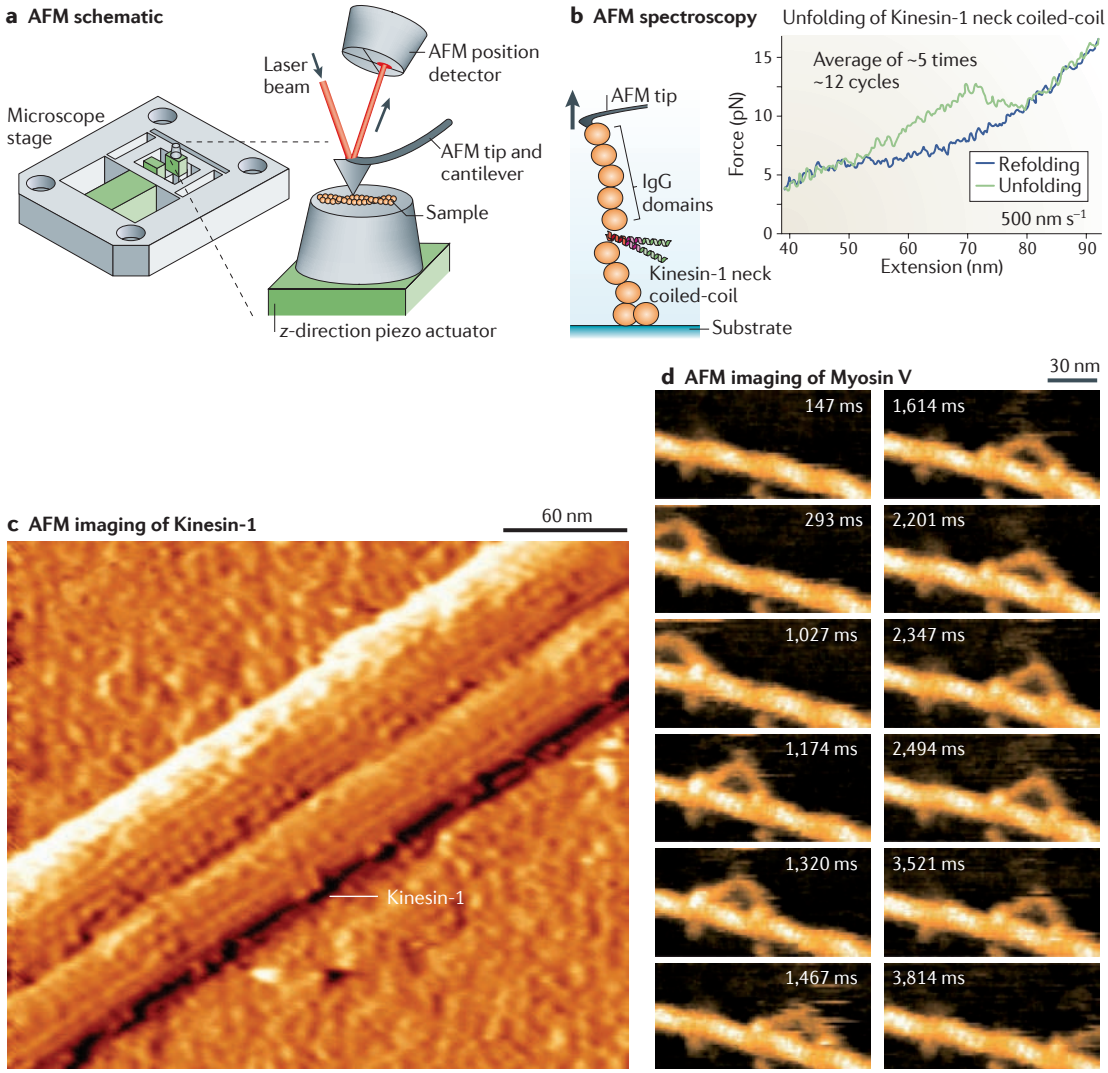

Figure 2 | **Using AFM to study single motor proteins. a** | Schematic of high-speed atomic force microscopy (AFM) to scan the height profile (z-axis) of single biomolecules at ~80 ms per frame. The sample is mounted on a piezo actuator (shown in green) that is attached to the microscope stage. The cantilever is driven to oscillate up and down near its resonance frequency by the piezo actuator. The cantilever tip intermittently taps the sample surface as it scans over it. Interaction forces between the tip and the sample deflect the tip. This is detected by a laser beam, which is reflected from the back of the AFM tip and directed onto a position detector. **b** | Depiction of AFM force spectroscopy applied to study the unfolding of the Kinesin-1 neck coiled-coil. Immunoglobulin G (IgG) domains are used as handles to link the two strands of the coiled-coil to the substrate surface and to the AFM tip. By pulling the tip upwards and downwards, the coiled-coil is pulled apart and released again. The force–extension curves of coiled-coil unfolding (green trace) and refolding (blue trace) were measured and are shown in the graph. The cantilever pulling rate was 500 nm sec^{-1}. **c** | An AFM image, recorded in tapping mode, of microtubules with single Kinesin-1 motors attached in the presence of the ATP analogue AMP-PNP, which stops motors on their tracks. **d** | A series of consecutive high-speed AFM images of myosin V, loosely attached sideways to the surface of the experimental chamber and imaged stepping along actin over about 4 s. Frame times are indicated. Figure in part **a** is modified, with permission, from REF. 187 © (2005) The Surface Science Society of Japan. Figure in part **b** is modified, with permission, from REF. 79 © (2009) National Academy of Sciences. Figure in part **d** is reproduced, with permission, from REF. 84 © (2010) Macmillan Publishers Ltd. All rights reserved.

picomolar to nanomolar concentrations of fluorescent molecules (FIG. 3). A priori knowledge (for example, knowing that the imaged object is a single molecule) makes it possible to obtain resolution beyond the conventional diffraction limit of the microscope[86,87–91]. High dilution of the fluorophores can be a problem if the required concentration of the interacting binding partner of the single molecule is micromolar, as is the case for the nucleotides that bind to motor proteins. This problem has been addressed using arrays of 'zero-mode waveguides', which consist of sub-wavelength holes in a metal film[92]. Single fluorophores inside the holes can be detected in the presence of micromolar concentrations of fluorophores outside the holes. This approach has been used to study DNA polymerase at the single-molecule level[92] but it has not yet been applied to cytoskeletal motors.

Piezo actuator
A piezoelectric crystal driven by a DC voltage to perform length changes in the Ångström to micrometre range.

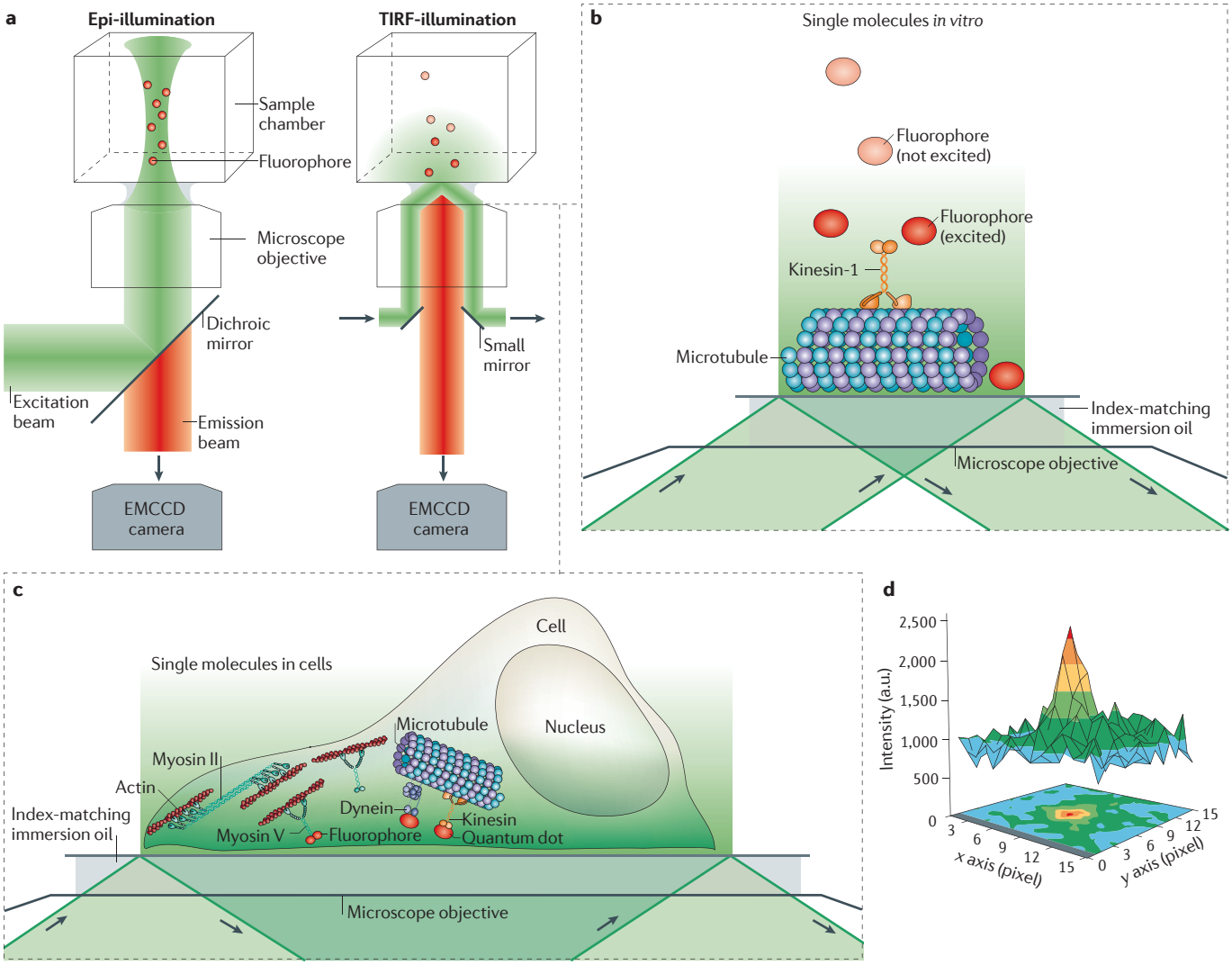

Figure 3 | **Single-molecule fluorescence microscopy to study motor proteins. a** | Epi-illumination (left) and total internal reflection fluorescence (TIRF) illumination (right) are shown. The excitation beam (shown in green) and backwards-emitted fluorescent light (shown in red) are separated by a dichroic mirror in the case of epi-illumination, and by a dichroic mirror or small mirrors at the edge of the objective in the case of TIRF illumination. An electron-multiplying charged coupled device (EMCCD) camera is used for low noise imaging at low light levels (for example, for detecting single fluorophores). **b** | TIRF concentrates the illumination light to a thin layer near the surface. Single fluorophores that are attached to kinesins moving along surface-attached microtubules can be excited and imaged selectively while fluorophores in the background, further away from the surface, remain unexcited. **c** | When applied to cells, TIRF only illuminates a thin layer where cells are attached to the surface of the chamber. Again, only the fluorophores near the surface of the chamber are excited and detected. Large numbers of motors are active in cells, as schematically indicated, but only those near the surface will be visible. **d** | A two-dimensional intensity profile of an image of a single deac-aminoADP (a fluorescent ADP analogue) attached to a cover slip. The maximum of the intensity clearly peaks over the background noise. The centre of the maximum, and thus the location of the fluorophore, can be determined with an uncertainty limited by the standard error of the mean of the distribution. a.u., arbitrary units. Figure in part **d** is reproduced, with permission, from REF. 63 © (2008) Macmillan Publishers Ltd. All rights reserved.

For the fluorescent imaging of single motors *in vitro* and in cells, probes need to be attached to motors. Probes can be synthetic fluorophores, fluorescent semiconductor nanoparticles (quantum dots) or recombinant fluorescent fusion proteins, such as green-fluorescent protein (GFP) and related proteins, which are co-expressed with the motor molecules[52,93]. Alternatively, non-fluorescent particles that scatter light, such as colloidal gold or silver particles, can be used[94]. Although non-fluorescent, scattering labels can be imaged with dark-field microscopy[95,96], fluorescent probes are mostly visualized with total internal reflection fluorescence (TIRF) microscopy[52,54,97] to reduce background and improve the signal-to-noise ratio (FIG. 3). Details of the resolution limit of fluorescence microscopy and applications in the broader single-molecule field have been discussed in recent reviews[52,54] (see also BOX 1).

Quantum dot
A nanometre-sized fluorescent semiconductor particle, the fluorescent properties of which depend on its shape and size.

Box 1 | **Resolution limits of single-molecule fluorescence microscopy**

The trajectories of single fluorophores attached to motors *in vitro* and in cells can be tracked with millisecond temporal resolution and nanometre spatial resolution using lasers for excitation and charged coupled device (CCD) cameras for detection. This resolution is sufficient to resolve the stepwise motion of single motor proteins. However, there is still little information on motor dynamics at the sub-millisecond timescale. A single fluorophore is imaged by the microscope as a diffraction-broadened spot (FIG. 3d). The centre of this spot (δx) can, in principle, be determined with arbitrary precision[180] with a remaining uncertainty δx:

$$\delta x = \frac{\lambda}{2\,NA\sqrt{N}}$$

where λ is the wavelength of the emitted light, *NA* is the numerical aperture of the microscope and *N* the number of photons counted. This applies when counting noise from detecting photons is limiting[181]. The problem of the correct fitting routine to describe the diffraction-broadened spot has been recently discussed in detail[119]. If, on the other hand, background noise (for example, out-of-focus fluorescence or camera readout noise) is limiting, the resolution scales with the inverse of the number of photons. With controlled background fluorescence and optimized magnification (when the pixel size of the detector is about equal to the width of the point spread function[181]), positional and temporal resolution are mostly limited by the number of collected photons at short timescales, and by baseline drift, the speed of moving molecules and photobleaching at longer timescales[54]. The limitations to resolution are thus well known, and these limitations are expected to be overcome, in part, when brighter and more stable fluorescent labels are available.

What recent developments have occurred? Small synthetic fluorophores are constantly being improved[182] and often outperform recombinant fluorescent proteins. Nanodiamonds can emit bright fluorescence at 550–800 nm[183,184], they do not blink over milliseconds, they show reduced photobleaching, they are non-cytotoxic and they can be functionalized to bind to proteins or DNA. Single-walled carbon nanotubes are a novel type of fluorescent probe and seem to be ideal labels, showing no bleaching, no blinking and fluorescence in the infrared[185].

Centroid tracking of single fluorophores. TIRF-microscopy data can be evaluated by centroid tracking, which refers to the reconstruction of the trajectory of the centre of the blurred image of a single fluorophore from a recorded video. This approach provided the first direct demonstration of the hand-over-hand processive stepping mechanism of single myosin V and Kinesin-1 molecules (FIG. 1C). With ~10^4 photons collected per second from a single cyanine dye, Cy3, attached to one head of the dimeric motors, the head could be localized with ~0.5 s temporal and ~1 nm spatial resolution over time periods of ~1 min[72,73,98]. Variations of this method have been introduced to further characterize the movement of single motors along their tracks *in vitro*. With two different cyanine dyes or quantum dots attached to the two heads of myosin V, heads could be colocalized with ~6–10 nm accuracy, providing further support for the hand-over-hand mechanism of processive movement[74,99]. In a similar approach, the broadly distributed step size of myosin VI was attributed to a mixture of large and small steps with narrow distributions[100]. Rotational movement of the myosin V motor heads during processive movement was shown in TIRF microscopy experiments in which the motor was fixed at the cargo-binding domain and a fluorescently labelled actin filament was transported by the motor heads. During each 36 nm step, the actin filament was found to randomly rotate by 90° both clockwise and counter-clockwise, consistent with a thermal twist in the myosin V neck during processive movement[101].

Fluorophores eventually photobleach, which means that they become non-fluorescent through light-induced chemical modification. This limits the time over which single fluorophores can be followed. However, photobleaching can be exploited to accurately localize single fluorophores in close proximity[102,103]. By sequential bleaching, distances of ~10 nm between single fluorophores attached to the heads of artificially dimerized myosin VI[104] could be resolved without the need for distinguishable colours. Single-molecule FRET (smFRET[52]) was similarly used to detect distances of <10 nm between donor dye (Cy3) and acceptor dye (Cy5) attached to the two heads of Kinesin-1 (REF. 105). In this experiment, the sensors were attached either to both kinesin heads at the neck linker or to one head at the tip and the other head at the base of the catalytic domain. The results suggest that Kinesin-1 has both heads bound to the microtubule at saturating ATP concentrations; at low ATP concentrations, when nucleotide binding becomes rate limiting, the motor is attached to the microtubule with a single head until ATP binds.

Spatial orientation of single fluorophores. Fluorescence can also be used to determine the spatial orientation of a fluorophore and the labelled molecule. When out of focus, the observed fluorescence-intensity pattern depends on the fluorophore's three-dimensional (3D)-orientation[106]. This fact was exploited to monitor the orientation of the myosin V lever arm during processive movement. The image plane was toggled between focused, for measuring motor head position, and defocused, for determining lever-arm orientation[107]. The lever arm was shown to rotate by about 70°, consistent with the 36 nm steps of the motor. Orientation and rotation of motor subdomains can also be studied at high time resolution if the polarizations of the excitation and emission beams are evaluated[52]. The fluorophore must be rigidly attached to the protein, and it is not possible to measure the orientation of the fluorophore along the axes orthogonal to the polarization direction of the excitation beam[52]. Full 3D orientation can be measured by switching beam direction and using polarization in epi-illumination or TIRF mode. To study Kinesin-1, the fluorophore bis-sulphorhodamine (BSR) was attached at two points to the catalytic head domain, and the excitation beam was polarized alternatingly along four polarization axes[108]. This showed that the head of Kinesin-1 is most mobile when ADP is bound. These experiments were inspired by earlier studies on muscle, where native myosin light chains were partly exchanged for BSR-labelled ones to study the 3D orientation of the skeletal muscle myosin lever arms during fibre contraction[109]. Polarization studies on BSR-labelled light chains on the myosin V lever arm revealed that the latter tilts between two discrete angles during processive movement[110]. For these studies, the probes were excited successively by an evanescent wave in four different polarization states and the orientation of the probe was characterized in all three orthogonal spatial axes. The results provided direct 3D evidence for lever-arm rotation and were consistent with the hand-over-hand walking mechanism. A further possible method for monitoring orientation is

Total internal reflection fluorescence
Excitation of fluorescence by the evanescent light field of a laser beam that is totally internally reflected at an interface between a medium of higher and one of lower index of refraction.

Point spread function
The point spread function characterizes the diffractive properties of an imaging system and is equal to the image of a point source of light through this imaging system.

Epi-illumination
Microscope illumination through the objective, commonly used for fluorescence excitation.

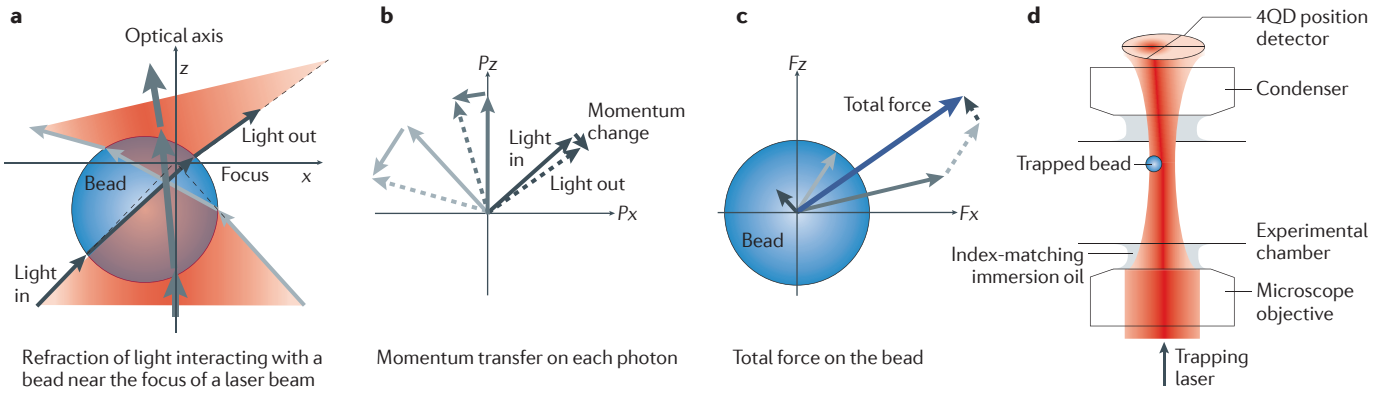

Figure 4 | **Optical tweezers to study single motor proteins. a** | Ray optics sketch of light rays within the laser light cone (shown in red) that impinge from different directions (indicated by light, medium and dark grey arrows) and are refracted through a bead trapped in optical tweezers. The bead is positioned slightly off the optical axis, and below the focus of a strongly focused laser. The width of the arrows indicates the light intensity, which is highest on the optical axis (as represented by the thickest arrow). **b** | The deflection of each photon results in a momentum change and a transfer of momentum onto the bead. The length of the arrows corresponds to the magnitude of momentum. As wavelength does not change, the magnitude of the momenta is unchanged by the deflection event (as indicated by the equal length of arrows). Arrows between solid (original photon momentum) and dashed (deflected photon momentum) arrows show the momentum transfers for individual photons out of the three rays of light, drawn in colours corresponding to part **a**. **c** | The total momentum transfer per time on all deflected photons in the three rays equals the force exerted on the bead (indicated by the blue arrow), which is the sum of the forces produced by the three rays. The gradient of intensity in the laser cone implies more photons per time impinging near the optical axis, that is, the dark grey arrow is longer. Here, the length of the arrows corresponds to the magnitude of force. **d** | The principle of high-bandwidth position and force detection by back-focal-plane interferometry using a quadrant photodiode (4QD position detector). The 4QD position detector is placed directly behind the microscope condenser so that it can collect the deflected laser light and detect angular shifts in the transmitted trapping light.

the use of visibly elongated probes. The rotation of the myosin V lever arm could be visualized by attaching short, rhodamine-labelled microtubules to its neck domain[111]. The results suggest that the forward swing of the neck of the leading myosin V head biases the random motion of the lifted head so that it eventually lands on the next binding site in the direction of motion.

A fundamental question about the basic mechanism of cytoskeletal motors, which can also be addressed by single-molecule fluorescence, concerns the coupling between the biochemical ATPase cycle and the mechanical conformations of the motor. The binding and dissociation of nucleotide from dimeric myosin V was visualized using the fluorescent nucleotide analogue deac-aminoATP[112]. The stepping of the motor along actin was simultaneously observed using Alexa-labelled calmodulin (the neck of myosin V binds light chains of the calmodulin family)[63]. The results showed that ADP dissociation from the trailing head is followed by ATP binding and a synchronous 36 nm step. Even at low ATP concentrations, the motor retained ADP in the lead head position when moving. Single-molecule fluorescence is therefore a very powerful tool, not only for the study of the global motion of motors but also for the tracking of intramolecular conformational changes and nucleotide binding.

Combining fluorescence and optical tweezers. Chemomechanical coupling can be studied by combining the use of fluorescence with optical tweezers. Optical tweezers exert piconewton forces and can be used to measure forces and displacements of the trapped microscopic probe particles (FIG. 4) (see below). The technical challenge in combining fluorescence imaging and optical tweezers is the detection of a minuscule fluorescence signal in the presence of the strong laser light needed for optical trapping. The trapping laser can cause background fluorescence of the trapped probe and enhanced photobleaching of the fluorophore. These problems were avoided by separating the trapping laser and the fluorophore in the focal plane by several micrometres when viewing the binding and release of fluorescently labelled nucleotides from single myosin II motor heads simultaneously with the mechanical interactions of these heads with actin[113]. These experiments showed that it is technically possible to monitor biochemistry and mechanics in a single experiment. This experiment is feasible even when the fluorophore is directly exposed to the optical-trap laser light if the dyes, laser wavelengths and filters are chosen carefully[114,115]. Photobleaching occurred in this situation mainly through the absorption of an infrared photon out of the excited state[114]. Enhanced photobleaching can also be avoided if trapping and fluorescence lasers are interlaced in time[116]. Owing to the technical challenges of combining fluorescence and optical tweezers, very few groups use this approach and many details of the chemomechanical coupling of molecular motors remain unexplored.

Light-scattering-based techniques. The problems of bleaching and blinking encountered with dyes can be avoided using colloidal silver or gold nanoparticles[96]. These particles scatter light efficiently and appear as bright spots against a dark background in dark-field illumination, such

Back-focal-plane interferometry
Laser interferometric detection of the displacement of optically trapped particles from the focus; uses imaging of the back focal plane of the microscope condenser, typically onto a quadrant photodiode.

Blinking
The switching of single fluorophores between bright and dark states, which hinders their use in time-resolved experiments.

that they can be tracked with sub-millisecond time resolution. Gold nanoparticles of ~40 nm in diameter were attached to the lever arm of myosin V and tracked during the motor's hand-over-hand processive forward movement with a time resolution of ~300 μs[95]. The results suggest that the unbound head rotates freely about the lever arm junction during a forward step, which might facilitate the motor's movement through dense actin meshworks. Another approach, called travelling-wave tracking (TWT)[66], uses a rapidly moving pattern of laser interference fringes to illuminate and track small polystyrene beads. Phase and amplitude of the regularly blinking scattered light can be detected so accurately that nanometre spatial and microsecond temporal resolution is possible. This technique was used to track polystyrene beads bound to dimeric myosin V[66], and revealed small axial and radial motions during the motor's processive forward steps along a surface-immobilized actin filament. Smaller probe sizes would improve temporal resolution, but particles need to exceed ~40 nm diameter to be distinguishable from the background[117]. Gold particles with diameters of 2–3 nm can, however, be tracked using a photothermal imaging technique[117] that is insensitive to the scattering background. Absorption of laser light, even by very small gold particles, gives rise to an increase in temperature around the illuminated particle. This can be detected by polarization interference contrast[117]. This technology for single-molecule localization with nanometre-sized probes is especially attractive for imaging over long periods of time but has yet to be applied to motor proteins.

Analysis tools for motor tracking

To understand how ensembles of molecular motors cooperate in cells, it is useful to start with *in vitro* experiments that go beyond the single-molecule level and analyse the movement of dimers or small ensembles of motors. Data must typically be analysed statistically, and this requires automated analysis tools to deal with large data sets.

***Tracking cytoskeletal motors* in vitro.** To analyse the movement of single and multiple motor proteins labelled by fluorophores in complex environments, specialised data analysis tools have been developed. Examples include the construction of kymographs, which monitor the time course of fluorescence intensities along a single axis in space, and the automated 2D or 3D tracking of single fluorophores by fitting 2D Gaussian bell curves to the diffraction-limited intensity distributions recorded from them[118,119] (FIG. 3d). The diffusive motion of several kinesins, including Kinesin-13 (REF. 120), Kinesin-3 (REFS 121,122) and Kinesin-1 (REF. 123), and of myosin motors[124,125] has been observed using these types of data analysis tools, as has the length-dependent microtubule depolymerization carried out by Kinesin-8 (Kinesin-8 diffuses along microtubules to depolymerize their ends)[126]. Furthermore, tracking of microtubule-crosslinking proteins and other motors has provided new insight into how these proteins move along, and regulate, microtubules. Tracking the yeast microtubule-crosslinking protein anaphase spindle elongation 1 (Ase1) made it possible to follow its diffusion and microtubule-crosslinking activity[127]. In the mitotic spindle, kinesins of opposite directionality act between overlapping microtubules and create a 'push–pull-muscle'. The homotetrameric Kinesin-5 was shown to crosslink microtubules in the mitotic spindle[128], preferentially in an antiparallel orientation[129], and to move the antiparallel microtubules apart. Single-molecule trajectories revealed that Kinesin-5 moves along microtubules in a directional, ATP-dependent mode, and a diffusive, ATP-independent mode[130,131]. The transition from diffusive to directional movement in physiological buffer conditions was shown to be triggered by binding between two microtubules; this implies a possible regulatory mechanism for Kinesin-5 in the mitotic spindle[132].

Tracking cytoskeletal motors in live cells. To monitor single motor proteins in live cells, several problems must be overcome. One is the background noise that is introduced by the presence of cellular autofluorescence resulting from flavinoids[133]. Another is that motors are found in high local concentrations and move quickly and in three dimensions. To overcome these problems, it is necessary to determine the trajectories of individual motors with at least millisecond time resolution. The resolution limits in the detection of single fluorophores are discussed in BOX 1. The various forms of super-resolution microscopy that are being developed[86] are typically not fast enough to follow motors or are based on the stochastic switching of fluorophores between excited and dark states, which also prevents tracking.

However, single fluorophores can be imaged in cells, in a thin layer near the surface, using TIRF microscopy. Trajectories recorded in TIRF mode have been analysed manually, frame-by-frame[134], which is time consuming and prone to bias. The methods used for the automated tracking of single molecules *in vitro* can also be used in cells[118,119]. They have revealed, for example, the on-rate, detachment-rate and the average residency-time of myosin X tail domains in the plasma membrane[135]. Very limited movement of the membrane-bound myosin X tail domains was found, suggesting that these domains are either bound to the cytoskeleton or corralled in a lipid compartment.

The problem of background noise can be overcome by using clusters of fluorophores. Single organelles, such as peroxisomes, that were labelled with ~1,000 fluorescent GFP molecules, or endocytosed vesicles containing many quantum dots, could be tracked as the cargo of molecular motors *in vivo*[136,137]. In these experiments, evidence was reported for steps of 8 nm, which is typical for a single kinesin or dynein motor *in vitro*. However, even *in vitro*, cargo movement by multiple motors has been found to involve fractional steps; in other words, variable step sizes that are smaller than 8 nm[138]. Thus, the question of whether or how multiple motors coordinate their steps during cargo movement remains open.

In addition to fluorescent-protein-based labelling, external probes with superior photophysical properties have been introduced into cells. Quantum-dot-labelled myosin V motors were incorporated into HeLa and COS-7 cells by spontaneous endocytosis. Subsequent osmotic shock treatment was required to break up the

Polarization interference contrast
A technique that is similar to differential interference contrast and that allows the sensitive detection of slight optical phase changes, induced by local heating owing to an absorbing nanoparticle, by interference with a slightly offset reference beam.

Kymograph
A graphical representation of movement along one axis over time, assembled by laterally adjoining linear slices out of consecutive video frames.

Gaussian bell curve
The most common probability density function of a random variable, defined by

$$f(x) = \frac{1}{\sqrt{2\pi\sigma^2}} \frac{(x-\mu)^2}{2\sigma^2}$$

where μ is the mean and σ^2 is the variance of the distribution.

encapsulating vesicles[139,140]. The movement of most of the quantum dots was random in direction, which could be the result of motors moving processively along random actin networks[140]. Another approach used genetically engineered tandem citrine tags, with high quantum-yield and stability and low bleaching, to label single kinesin molecules inside cells. Citrine is derived from enhanced yellow fluorescent protein (EYFP). Tracking individual citrine-tagged Kinesin-1 motors in cells showed that their speed and processivity agreed well with *in vitro* results[141]. Thus, the first steps necessary to perform single-molecule experiments with motors in cells have been taken, but further advances are necessary to be able to broadly apply this approach.

Studying motors with optical tweezers

Optical tweezers are an all-optical non-contact tool, based on a strongly focused laser beam, that can be combined with high-resolution light microscopy to measure piconewton forces and nanometre displacements of micron-sized refractile objects after they are trapped near the focus of the laser light. This parameter range is suitable for quantitatively studying the production of force by, and movement of, motor proteins[142].

The fundamental principles and the technical implementations of optical tweezers to study single proteins or nucleic acid molecules are well established and extensively reviewed[53,54,143,144]. In the following sections, we remind the reader of some of the fundamental limitations of optical tweezers, in terms of spatial and temporal resolution, that must be kept in mind when performing single-molecule mechanical experiments on motor proteins. We also discuss recent developments and technological refinements in the use of optical tweezers that bring about new opportunities to investigate molecular motors *in vitro*, and *in vivo* in cells or whole organisms.

Measuring the force of molecular motors. Feedback-enforced position-clamping in optical tweezers experiments has been used to measure the isometric forces of myosin motors. This was first introduced for the 'three-bead assay' (FIG. 5), which was used to measure the power strokes of non-processive skeletal muscle myosin II[18,43,145]. A myosin three-bead assay consists of two beads held in tweezers and used to suspend an actin filament while a substrate-attached third bead is used as a pedestal for a myosin motor. Initially, the same bead that was used to measure bead position, and thus the myosin power stroke, was also used to measure force. This geometry cannot provide truly isometric conditions as there are compliant linkages between the motor and the beads[146–149]. The linkage between the actin filament and the beads at either end is especially crucial. The linkage compliance can be measured both by detecting correlated thermal fluctuations between the beads[147] and by oscillating one bead and observing the other[149]. The compliance was found to be highly nonlinear, and it can be very soft unless substantial pre-tension is put on the bead–filament–bead 'dumbbell'[148,150]. With all of these linkage compliances, the motor will move even if the bead used to measure position and force is kept at a fixed position. This problem can be avoided when one bead is used to measure force and the other bead is kept at a fixed position[151], ensuring that sufficient pre-tension on the actin filament is maintained[148].

Displacement measurements of molecular motors. Pure displacement measurements are made with force clamps. The displacement of the bead with respect to the centre of the optical tweezers (x) is held constant by feedback, so that a constant trap force is balanced by a constant force that is exerted by the motor on the trapped bead. This is achieved by rapid (microsecond) steering of the tweezers beam using acousto-optic[18,152] or electro-optic modulators[153]. Force clamps have been applied to accurately measure the force–velocity curves of motor proteins and to study mechanochemical coupling for processive kinesins and myosin V in 'single-bead assays'[75,77,154–157] (FIG. 5a), as well as for measuring RNA polymerase processing on a DNA template[158]. An all-optical force clamp, which avoids any electronic feedback and opposes strong and weak optical tweezers, has been developed by the Block laboratory[159]. In this method, two beads that are coupled, for example, by a strand of DNA, are held so that the bead in the weaker tweezers is pulled to the top of the trapping potential, where the force levels off and becomes constant. In this manner, the energy landscapes of DNA and RNA folding were accurately mapped[160–162].

An elegant force-clamp experiment was used to test whether one or both heads of Kinesin-1 are bound to the microtubule in-between processive steps (FIG. 5a). One of the heads was tethered by a stretch of DNA to a trapped bead. This bead was used to apply rapidly alternating hindering and assisting loads on the motor head. The displacements of the bead indicated that the linked head alternated between a bound and an unbound state during processive stepping[75].

Temporal resolution of optical tweezers assays. In discussing the physical limits of time resolution, one needs to distinguish two experimental scenarios — that is, the investigation of processive motors and of non-processive motors. For processive motors, details such as the conformational changes of the motor head in the attached state (for example, sub-steps in the processive motion) need to be resolved. For non-processive motors, the instant that the motor binds to the actin or microtubule needs to be detected before details of conformational changes can be looked at. In addition, when applying feedback loops to control the position of the optical tweezers, one needs to know how fast the feedback can be engaged. Generally, the viscous drag and the elastic stiffness of the tweezers and the molecules involved determine the response time of the trapped bead[163,164]. In the case of the highly processive and comparably stiff motor Kinesin-1, time resolution of ~15 ms could be achieved[154], and this made it possible to prove that there is tight coupling between ATP hydrolysis and motor steps. An even higher time resolution of ~1 ms has been achieved using small (200 nm diameter) beads in the tweezers. This helped to detect sub-steps in the motion of the processive myosin, myosin V[65].

Isometric force
The force that is generated by a muscle contracting without changing length.

Trap force
The force that is imposed by optical tweezers on a trapped particle.

Viscous drag
The frictional force on objects moving in a viscous fluid. The viscous drag force is proportional to the velocity of the moving object. For small spherical objects moving slowly through a viscous fluid (that is, at a low Reynolds number) the viscous drag coefficient is $\beta = 6\pi\eta r$, where r is the Stokes radius of the particle and η the viscosity of the fluid.

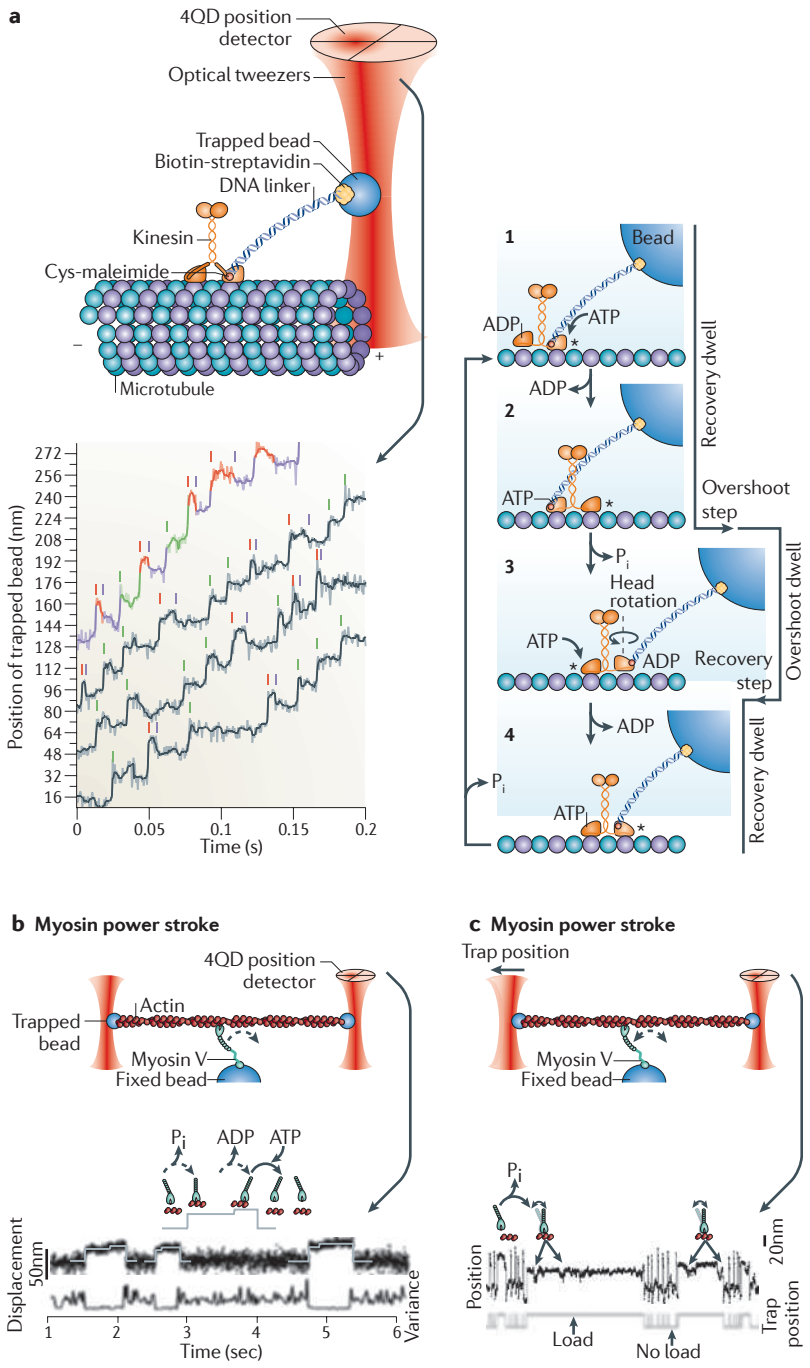

Figure 5 | **Optical tweezers to study movement of dimeric motors and power strokes of single motor heads.** **a** | 'Single-bead assay' to study the 'processive' stepping of Kinesin-1, with a load applied to one of the kinesin heads. One head is tethered by a DNA linker to a bead held in an optical trap. The displacement traces (recorded with an assisting load of 1.7 pN) show the position of the trapped bead and the 16 nm stepping pattern of the tethered head. Traces can be interpreted with the help of the schematic sequence of motor states shown in steps **1**–**4**. The starting position (step **1**) shows the tethered head without nucleotide (indicated by an asterisk) and strongly bound to the microtubule, just before the binding of ATP. ATP binding causes neck-linker docking and brings the ADP-bound trailing head forward. ADP release from this head follows after binding to the microtubule (step **2**). This all occurs without bead movement. Detachment of the tethered head from the microtubule and its forward movement then actually generates bead displacement 'overshoots' (step **3**), marked by orange vertical bars above the traces, before the head rebinds to the microtubule in the recovery step (step **4**), marked by purple bars above the traces. This demonstrates the 'hand-over-hand' stepping mechanism of Kinesin-1. With this approach, the effect of load on a single head during processive stepping of Kinesin-1 can be studied. **b** | The 'three-bead assay' uses two optical traps, each holding a bead, to suspend an actin filament over a single myosin V motor head that is attached to the third bead. Position detectors record individual power strokes, which are bi-phasic in the case of myosin V. The displacements of the trapped beads from the trap centres indicate the position of the actin filament. The displacement data show intervals of decreased variance that indicate myosin binding to actin and the two consecutive power strokes (dashed arrows). The bigger sub-step of the power stroke is coupled to inorganic phosphate (P_i) release and the smaller one is coupled to ADP release, as shown in the schematic. **c** | Here, real-time detection of myosin binding is used to control the position of the traps and to rapidly apply load to myosin following the binding event. This design has been used to provoke reversals of the main power stroke of myosin V (as indicated by the arrows on the displacement records) and to demonstrate reversibility in the chemomechanical cycle of myosin. 4QD, quadrant photodiode. Figure in part **a** is modified, with permission, from REF. 75 © (2009) Macmillan Publishers Ltd. All rights reserved. Figure in part **b** is modified, with permission, from REF. 61 © (2002) Macmillan Publishers Ltd. All rights reserved. Figure in part **c** is modified, with permission, from REF. 67 © (2010) Macmillan Publishers Ltd. All rights reserved.

Methods for detecting the binding of non-processive motors in three-bead assays were pioneered in studies on muscle myosin[43,149]. Binding of the motor to the filament causes a change in the overall stiffness of the system (κ) which can be monitored as a change in displacement variance of the trapped beads ($\langle x^2 \rangle$) with the Boltzmann constant k_B:

$$\frac{1}{2}\kappa\langle x^2\rangle = \frac{1}{2}k_B T$$

because the two quantities are directly related to each other via the temperature (T). Early experiments with myosin achieved a time resolution of tens of milliseconds and showed that the power stroke of myosin was only about 5 nm[43,149]. The various elastic compliances in the three-bead myosin assay system were later quantified and pre-tension was used in the suspended actin filament to increase time resolution[149]. In later three-bead assays with the Kinesin-14 NCD[45], the time resolution was estimated by numerical simulations to be ~15 ms. Theory showed that time resolution for detecting motor binding is limited by the ratio of the variances before and after binding[165]. With careful optimization, a resolution of ~5 ms was reached in a myosin assay[165]. Using the same approach, ~300 µs resolution was achieved for a muscle myosin assay[166]. By moving both tweezers back and forth with a constant velocity in a myosin three-bead assay, all

Boltzmann constant
This constant relates the average thermal energy of a microscopic particle to temperature.

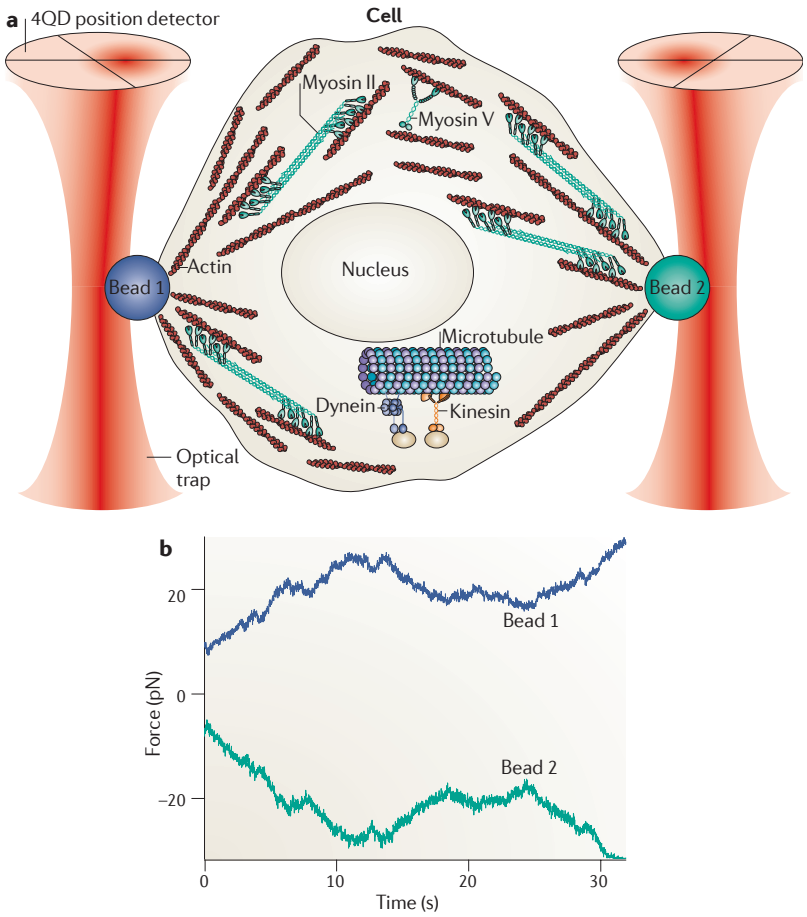

Figure 6 | **Optical tweezers used to measure force fluctuations of cells. a** | Sketch of a cell suspended between two optically trapped beads, with the internal force-generating structures of actin and myosin depicted. Force measurements on suspended cells make it possible to measure the total force that is generated by a single cell. **b** | Time trace of the force fluctuations exerted on bead 1 and bead 2. Data were recorded from an MLO-Y4 osteocyte using beads of 4 µm diameter. The forces exerted on both beads appear to largely balance each other. This suggests that intracellularly generated forces, that is, forces generated by the cytoskeleton, are predominant. 4QD, quadrant photodiode. Figure in part **b** is modified, with permission, from REF. 178 © (2009) The American Physical Society.

of the compliances that attenuate amplitudes and limit time resolution could be quantified[167].

For less stiff motors, such as non-muscle myosins, time resolution can be improved by applying small-amplitude forced oscillations in the kHz range on one of the trapped beads[64]. With a resolution of ~1 ms, using an ensemble-averaging technique, it was found that myosin class I produces a working stroke in two sub-steps, which are probably coupled to the release of inorganic phosphate and ADP[64]. Similar observations have since been made for other myosin isoforms, specifically classes I, II, V and VI[61,68,69,166,168,169]. Fast detection of myosin binding can also be used to trigger a rapid application of load, subsequent to binding, by moving the optical tweezers[67–69]. Combined again with ensemble averaging, the load-dependence of the two sequential phases of the working stroke could be resolved for smooth muscle myosin II and myosin V[68,69]. Recently, it was also directly shown that the myosin V power stroke is reversible under a large enough load[67]. Observing such events was made possible by rapid detection of attachment, which then triggered application of load. Further evidence for power-stroke reversal comes from the finding of asymmetric rupture forces of the motor from actin[170], whereas off-axis loads have little effect on rupture forces and ADP affinity[171]. Asymmetric rupture forces — different forces required to detach a motor from its track when the motor is pulled in a forward or backward direction — were also reported for dimeric Kinesin-1. In these experiments, it was shown that the affinity of kinesin for ADP is regulated by loading direction[172]. These characterizations of motor mechanics under load *in vitro* are crucial for understanding how motors perform in the cellular context, when their cargo is exposed to constantly changing forces.

Using optical tweezers in cells. The selective and controlled optical trapping of particles, vesicles or organelles inside cells is difficult because of the high index of refraction of many intracellular objects that will indiscriminately assemble in the trap. A further complication for a quantitative application of tweezers is the fact that calibration of force and displacement are not as straightforward in cells as they are in buffer. Ashkin *et al.*[173] trapped mitochondria in the amoeba *Reticulomyxa* spp. in the early days of optical tweezers and roughly estimated the force generated by a single motor to be ~2.7 pN, which is remarkably close to the true force. For mechanical characterization of motors in cells using optical tweezers, it seems best to use either distinctive indigenous cellular particles with a high index of refraction, such as lipid droplets, or injected or ingested particles that are clearly identifiable, such as gold beads. The tracking and trapping of lipid droplets revealed that the motors that transported these droplets in basal and apical directions in early *Drosophila melanogaster* embryos had unitary stall forces of ~1.1 pN[174]. The tweezers were calibrated approximately by extracting droplets from the embryos and comparing trap force to viscous drag for a given droplet size. The initial force estimate was revised to ~2.6 pN in a later report on the same system[175].

The use of gold, or other particles that can resonantly absorb light of a certain wavelength, to investigate motor mechanics in cells still needs to be explored but is promising for two reasons. First, such particles are strongly scattering. When they are too large or are illuminated exactly at resonance, these particles will absorb light, will not be trappable and will heat up rapidly. Second, when a wavelength near, but not on, resonance is used, the trapping force is predicted to be up to 50-fold enhanced[176]. This effect, which should occur near any sharp resonance, might make it possible to trap particles specifically inside cells.

Motors can, in some cases, also be studied by optical tweezers 'reaching through' the cell membrane, with the trapped bead on the outside of the cell, such that calibration is not a problem. The anterograde and retrograde movements of beads attached to the outside of *Chlamydomonas* spp. flagella were observed in this manner[177]. When beads are attached to the outside of cells, single motors cannot normally be detected, but one can

record the sum of the activity of the many motors inside the cell. If one suspends a cell by two attached beads, the collective motor activity typically results in negatively correlated random fluctuations of the beads (FIG. 6). Interestingly, it was found that the force transmitted to the beads increases significantly with increased trap stiffness[178]. Very similar behaviour had been observed before in an actin–myosin *in vitro* model system[179]. Although optical tweezers have thus been a very powerful tool to characterize motor proteins *in vitro*, their use in cells has delivered promising results but still poses challenges.

Concluding remarks

Since the first single-molecule experiments over 20 years ago, there has been a dramatic development of the field. The single-molecule approach has made it possible to study the basic mechanisms of many cellular machines, in particular the motors of the cytoskeleton, and also DNA- and RNA-based motors involved in transcription and translation, as well as the rotary motor F_1-ATPase. In a powerful combination with molecular biology and structural studies, dynamic single-molecule techniques have revealed many details of mechanochemical energy transduction and have 'breathed life' into atomic resolution structures. Yet, many critical issues still need to be addressed; most prominently, the function and regulation of motors in the complex cellular context. This poses a challenge to the field to further develop, combine and adapt single-molecule technologies. The development of optimized long-lived fluorescence dyes with emission wavelengths far from the background, for example in the near-infrared, will be important progress. Furthermore, it is foreseeable that various new nanoparticles will be manipulated to enter the cell combined with specific attachment and recognition chemistry to serve both as fluorescent probes and as handles for manipulation by optical tweezers. With such capabilities, we will eventually be able to follow our 'actors', molecule by molecule, attending to their 'daily business' in their native environment.

1. Howard, J. *Mechanics of Motor Proteins and the Cytoskeleton* (Sinauer Associates Inc., Sunderland, Massachusetts, 2001).
2. Hirokawa, N., Noda, Y., Tanaka, Y. & Niwa, S. Kinesin superfamily motor proteins and intracellular transport. *Nature Rev. Mol. Cell Biol.* **10**, 682–696 (2009).
3. Kardon, J. R. & Vale, R. D. Regulators of the cytoplasmic dynein motor. *Nature Rev. Mol. Cell Biol.* **10**, 854–865 (2009).
4. Spudich, J. A. & Sivaramakrishnan, S. Myosin VI: an innovative motor that challenged the swinging lever arm hypothesis. *Nature Rev. Mol. Cell Biol.* **11**, 128–137 (2010).
5. Verhey, K. J. & Hammond, J. W. Traffic control: regulation of kinesin motors. *Nature Rev. Mol. Cell Biol.* **10**, 765–777 (2009).
6. Vicente-Manzanares, M., Ma, X. F., Adelstein, R. S. & Horwitz, A. R. Non-muscle myosin II takes centre stage in cell adhesion and migration. *Nature Rev. Mol. Cell Biol.* **10**, 778–790 (2009).
7. Kull, F. J. & Endow, S. A. Kinesin: switch I & II and the motor mechanism. *J. Cell Sci.* **115**, 15–23 (2002).
8. Geeves, M. A. & Holmes, K. C. in *Advances in Protein Chemistry* Vol. 71 (*Fibrous Proteins: Muscle and Molecular Motors*) 161–193 (Elsevier Academic Press Inc., San Diego, 2005).
9. Kikkawa, M. The role of microtubules in processive kinesin movement. *Trends Cell Biol.* **18**, 128–135 (2008).
10. Rice, S. *et al.* A structural change in the kinesin motor protein that drives motility. *Nature* **402**, 778–784 (1999).
A classic study that provides evidence for the kinesin neck linker conformational change by using electron paramagnetic resonance, FRET, kinetics and electron microscopy.
11. Rayment, I. *et al.* Three-dimensional structure of myosin subfragment-1: a molecular motor. *Science* **261**, 50–58 (1993).
Presented the first X-ray crystallography structure of a myosin motor domain, which strongly advanced our understanding of motor function.
12. Schröder, R. R. *et al.* Three-dimensional atomic model of F-actin decorated with *Dictyostelium* myosin S1. *Nature* **364**, 171–174 (1993).
13. Dominguez, R., Freyzon, Y., Trybus, K. M. & Cohen, C. Crystal structure of a vertebrate smooth muscle myosin motor domain and its complex with the essential light chain: visualization of the pre-power stroke state. *Cell* **94**, 559–571 (1998).
14. Houdusse, A., Kalbokis, V. N., Himmel, D., Szent-Gyorgyi, A. G. & Cohen, C. Atomic structure of scallop myosin subfragment S1 complexed with MgADP: a novel conformation of the myosin head. *Cell* **97**, 459–470 (1999).
15. Burgess, S. *et al.* The prepower stroke conformation of myosin V. *J. Cell Biol.* **159**, 983–991 (2002).
16. Walker, M. L. *et al.* Two-headed binding of a processive myosin to F-actin. *Nature* **405**, 804–807 (2000).
17. Sweeney, H. L. & Houdusse, A. Structural and functional insights into the myosin motor mechanism. *Annu. Rev. Biophys.* **39**, 539–57 (2010).
18. Finer, J. T., Simmons, R. M. & Spudich, J. A. Single myosin molecule mechanics-piconewton forces and nanometer steps. *Nature* **368**, 113–119 (1994).
Describes the three-bead single-molecule assay for myosin for the first time and is also the first report of myosin power strokes and single-molecule forces.
19. De La Cruz, E. M. & Ostap, E. M. in *Methods in Enzymology* Vol. 455, (*Biothermodynamics Part A*) (Eds Johnson, M. L., Holt, J. M. & Ackers, G. K) 157–192 (Elsevier Academic Press Inc., San Diego, 2009).
20. Zeng, W. *et al.* Dynamics of actomyosin interactions in relation to the cross-bridge cycle. *Phil. Trans. R. Soc. B* **359**, 1843–1855 (2004).
21. Marx, A., Muller, J. & Mandelkow, E. in *Advances in Protein Chemistry* Vol. 71 (*Fibrous Proteins: Muscle and Molecular Motors*) 299–344 (Elsevier Academic Press Inc., San Diego, 2005).
22. Sweeney, H. L. & Houdusse, A. in *Annual Review of Biophysics* Vol. 39 539–557 (Annual Reviews, Palo Alto, 2010).
23. Terrak, M., Rebowski, G., Lu, R. C., Grabarek, Z. & Dominguez, R. Structure of the light chain-binding domain of myosin V. *Proc. Natl Acad. Sci. USA* **102**, 12718–12723 (2005).
24. Bosch, J. *et al.* Structure of the MTIP–MyoA complex, a key component of the malaria parasite invasion motor. *Proc. Natl Acad. Sci. USA* **103**, 4852–4857 (2006).
25. Vinogradova, M. V., Malanina, G. G., Reddy, A. S. N. & Fletterick, R. J. Structure of the complex of a mitotic kinesin with its calcium binding regulator. *Proc. Natl Acad. Sci. USA* **106**, 8175–8179 (2009).
26. Li, H. L., DeRosier, D. J., Nicholson, W. V., Nogales, E. & Downing, K. H. Microtubule structure at 8Å Resolution. *Structure* **10**, 1317–1328 (2002).
27. Milligan, R. A., Whittaker, M. & Safer, D. Molecular structure of F-actin and location of surface binding sites. *Nature* **348**, 217–221 (1990).
28. Rayment, I. *et al.* Structure of the actin–myosin complex and its implications for muscle-contraction. *Science* **261**, 58–65 (1993).
29. Mandelkow, E. M., Mandelkow, E. & Milligan, R. A. Microtubule dynamics and microtubule caps: a time-resolved cryo-electron microscopy study. *J. Cell Biol.* **114**, 977–991 (1991).
30. Hirose, K., Lockhart, A., Cross, R. A. & Amos, L. A. Three-dimensional cryoelectron microscopy of dimeric kinesin and ncd motor domains on microtubules. *Proc. Natl Acad. Sci. USA* **93**, 9539–9544 (1996).
31. Burgess, S. A., Walker, M. L., Sakakibara, H., Knight, P. J. & Oiwa, K. Dynein structure and power stroke. *Nature* **421**, 715–718 (2003).
32. Bodey, A. J., Kikkawa, M. & Moores, C. A. 9-Ångström structure of a microtubule-bound mitotic motor. *J. Mol. Biol.* **388**, 218–224 (2009).
33. Thirumurugan, K., Sakamoto, T., Hammer, J. A., Sellers, J. R. & Knight, P. J. The cargo-binding domain regulates structure and activity of myosin 5. *Nature* **442**, 212–215 (2006).
34. Liu, J., Taylor, D. W., Krementsova, E. B., Trybus, K. M. & Taylor, K. A. Three-dimensional structure of the myosin V inhibited state by cryoelectron tomography. *Nature* **442**, 208–211 (2006).
35. Al-Bassam, J. *et al.* Distinct conformations of the kinesin Unc104 neck regulate a monomer to dimer motor transition. *J. Cell Biol.* **163**, 743–753 (2003).
36. Stock, M. F. *et al.* Formation of the compact confomer of kinesin requires a COOH-terminal heavy chain domain and inhibits microtubule-stimulated ATPase activity. *J. Biol. Chem.* **274**, 14617–14623 (1999).
37. Dietrich, K. A. *et al.* The Kinesin-1 motor protein is regulated by a direct interaction of its head and tail. *Proc. Natl Acad. Sci. USA* **105**, 8938–8943 (2008).
38. Lucic, V., Forster, F. & Baumeister, W. Structural studies by electron tomography: from cells to molecules. *Annu. Rev. Biochem.* **74**, 833–865 (2005).
39. Sheetz, M. P. & Spudich, J. A. Movement of myosin-coated fluorescent beads on actin cables *in vitro*. *Nature* **303**, 31–35 (1983).
40. Kishino, A. & Yanagida, T. Force measurements by micromanipulation of a single actin filament by glass needles. *Nature* **334**, 74–76 (1988).
41. Yanagida, T., Nakase, M., Nishiyama, K. & Oosawa, F. Direct observation of motion of single F-actin filaments in the presence of myosin. *Nature* **307**, 58–60 (1984).
42. Kron, S. J. & Spudich, J. A. Fluorescent actin-filaments move on myosin fixed to a glass surface *Proc. Natl Acad. Sci. USA* **83**, 6272–6276 (1986).
43. Molloy, J. E., Burns, J. E., Kendrick-Jones, J., Tregear, R. T. & White, D. C. S. Movement and force produced by a single myosin head. *Nature* **378**, 209–212 (1995).
A careful study of power strokes of single myosin dimers, which properly takes into account thermal fluctuations and gives the most accurate estimate of power-stroke amplitude.
44. Wendt, T. G. *et al.* Microscopic evidence for a minus-end-directed power stroke in the kinesin motor ncd. *EMBO J.* **21**, 5969–5978 (2002).
45. deCastro, M. J., Fondecave, R. M., Clarke, L. A., Schmidt, C. F. & Stewart, R. J. Working strokes by single molecules of the kinesin-related microtubule motor ncd. *Nature Cell Biol.* **2**, 724–729 (2000).
46. Endow, S. A. & Higuchi, H. A mutant of the motor protein kinesin that moves in both directions on microtubules. *Nature* **406**, 913–916 (2000).

47. Svoboda, K., Schmidt, C. F., Schnapp, B. J. & Block, S. M. Direct observation of kinesin stepping by optical trapping interferometry. *Nature* **365**, 721–727 (1993).
The first report on the steps and stall forces of single kinesin motors, which were measured by optical trapping.
48. Mehta, A. D. *et al.* Myosin-V is a processive actin-based motor. *Nature* **400**, 590–593 (1999).
49. Hirakawa, E., Higuchi, H. & Toyoshima, Y. Y. Processive movement of single 22S dynein molecules occurs only at low ATP concentrations. *Proc. Natl Acad. Sci. USA* **97**, 2533–2537 (2000).
50. Reck-Peterson, S. L. *et al.* Single-molecule analysis of dynein processivity and stepping behavior. *Cell* **126**, 335–348 (2006).
A landmark paper using quantum dots to perform single-molecule experiments with dimeric dynein, and showing processive stepping behaviour.
51. Toba, S., Watanabe, T. M., Yamaguchi-Okimoto, L., Toyoshima, Y. Y. & Higuchi, H. Overlapping hand-over-hand mechanism of single molecular motility of cytoplasmic dynein. *Proc. Natl Acad. Sci. USA* **103**, 5741–5745 (2006).
52. Joo, C., Balci, H., Ishitsuka, Y., Buranachai, C. & Ha, T. Advances in single-molecule fluorescence methods for molecular biology. *Annu. Rev. Biochem.* **77**, 51–76 (2008).
53. Moffitt, J. R., Chemla, Y. R., Smith, S. B. & Bustamante, C. Recent advances in optical tweezers. *Annu. Rev. Biochem.* **77**, 205–228 (2008).
54. Greenleaf, W. J., Woodside, M. T. & Block, S. M. High-resolution, single-molecule measurements of biomolecular motion. *Annu. Rev. Biophys. Biomol. Struct.* **36**, 171–190 (2007).
55. Block, S. M. Kinesin motor mechanics: binding, stepping, tracking, gating, and limping. *Biophys. J.* **92**, 2986–2995 (2007).
56. Gennerich, A. & Vale, R. D. Walking the walk: how kinesin and dynein coordinate their steps. *Curr. Opin. Cell Biol.* **21**, 59–67 (2009).
57. Sellers, J. R. & Veigel, C. Walking with myosin V. *Curr. Opin. Cell Biol.* **18**, 68–73 (2006).
58. Altman, D., Sweeney, H. L. & Spudich, J. A. The mechanism of myosin VI translocation an its load-induced anchoring. *Cell* **116**, 737–749 (2004).
59. Gennerich, A., Carter, A. P., Reck-Peterson, S. L. & Vale, R. D. Force-induced bidirectional stepping of cytoplasmic dynein. *Cell* **131**, 952–965 (2007).
Showed, in a single-molecule assay, that the processive myosin V motor takes a step in two phases and, further, that it needs a thermal fluctuation to reach its next binding site.
60. Svoboda, K. & Block, S. M. Force and velocity measured for single kinesin molecules. *Cell* **77**, 773–784 (1994).
61. Veigel, C., Wang, F., Bartoo, M. L., Sellers, J. R. & Molloy, J. E. The gated gait of the processive molecular motor, myosin V. *Nature Cell Biol.* **4**, 59–65 (2002).
62. Schnitzer, M. J. & Block, S. M. Kinesin hydrolyses one ATP per 8-nm step. *Nature* **388**, 386–390 (1997).
A landmark paper that proves, from the statistical analysis of single-molecule data, that kinesin uses one ATP molecule per 8 nm step.
63. Sakamoto, T., Webb, M. R., Forgacs, E., White, H. D. & Sellers, J. R. Direct observation of the mechanochemical coupling in myosin Va during processive movement. *Nature* **455**, 128–132 (2008).
64. Veigel, C. *et al.* The motor protein myosin-I produces its working stroke in two steps. *Nature* **398**, 530–533 (1999).
65. Uemura, S., Higuchi, H., Olivares, A. O., De La Cruz, E. M. & Ishiwata, S. Mechanochemical coupling of two substeps in a single myosin V motor. *Nature Struct. Mol. Biol.* **11**, 877–883 (2004).
66. Cappello, G. *et al.* Myosin V stepping mechanism. *Proc. Natl Acad. Sci. USA* **104**, 15328–15333 (2007).
67. Sellers, J. R. & Veigel, C. Direct observation of the myosin-Va power stroke and its reversal. *Nature Struct. Mol. Biol.* **17**, 590–595 (2010).
The first direct evidence that the myosin power stroke can be physically reversed, which has important implications for motor regulation in cells.
68. Veigel, C., Schmitz, S., Wang, F. & Sellers, J. R. Load-dependent kinetics of myosin-V can explain its high processivity. *Nature Cell Biol.* **7**, 861–869 (2005).
69. Veigel, C., Molloy, J. E., Schmitz, S. & Kendrick-Jones, J. Load-dependent kinetics of force production by smooth muscle myosin measured with optical tweezers. *Nature Cell Biol.* **5**, 980–986 (2003).
70. Kon, T. *et al.* Helix sliding in the stalk coiled coil of dynein couples ATPase and microtubule binding. *Nature Struct. Mol. Biol.* **16**, 325–333 (2009).
71. Asbury, C. L., Fehr, A. N. & Block, S. M. Kinesin moves by an asymmetric hand-over-hand mechanism. *Science* **302**, 2130–2134 (2003).
72. Yildiz, A. *et al.* Myosin V walks hand-over-hand: single fluorophore imaging with 1.5-nm localization. *Science* **300**, 2061–2065 (2003).
73. Yildiz, A., Tomishige, M., Vale, R. D. & Selvin, P. R. Kinesin walks hand-over-hand. *Science* **303**, 676–678 (2004).
74. Warshaw, D. M. *et al.* Differential labeling of myosin V heads with quantum dots allows direct visualization of hand-over-hand processivity. *Biophys. J.* **88**, L30–L32 (2005).
75. Guydosh, N. R. & Block, S. M. Direct observation of the binding state of the kinesin head to the microtubule. *Nature* **461**, 125–128 (2009).
76. Gebhardt, J. C. M., Clemen, A. E. M., Jaud, J. & Rief, M. Myosin-V is a mechanical ratchet. *Proc. Natl Acad. Sci. USA* **103**, 8680–8685 (2006).
77. Carter, N. J. & Cross, R. A. Mechanics of the kinesin step. *Nature* **435**, 308–312 (2005).
78. Engel, A. & Gaub, H. E. Structure and mechanics of membrane proteins. *Annu. Rev. Biochem.* **77**, 127–148 (2008).
79. Bornschlögl, T., Woehlke, G. & Rief, M. Single molecule mechanics of the kinesin neck. *Proc. Natl Acad. Sci. USA* **106**, 6992–6997 (2009).
80. Schaap, I. A. T., de Pablo, P. J. & Schmidt, C. F. Resolving the molecular structure of microtubules under physiological conditions with scanning force microscopy. *Eur. Biophys. J.* **33**, 462–467 (2004).
81. Schaap, I. A. T., Carrasco, C., de Pablo, P. J., MacKintosh, F. C. & Schmidt, C. F. Elastic response, buckling, and instability of microtubules under radial indentation. *Biophys. J.* **91**, 1521–1531 (2006).
82. Schaap, I. A. T., Hoffmann, B., Carrasco, C., Merkel, R. & Schmidt, C. F. Tau protein binding forms a 1 nm thick layer along protofilaments without affecting the radial elasticity of microtubules. *J. Struct. Biol.* **158**, 282–292 (2007).
83. Schaap, I. A. T. *et al.* Cytoskeletal filaments and their associated proteins studied with atomic force microscopy. *Biophys. J.* (Suppl) 309A (2007).
84. Kodera, N., Yamamoto, D., Ishikawa, R. & Ando, T. Video imaging of walking myosin V by high-speed atomic force microscopy. *Nature* **468**, 72–76 (2010).
85. Yamashita, H. *et al.* Tip-sample distance control using photothermal actuation of a small cantilever for high-speed atomic force microscopy. *Rev. Sci. Instr.* **78**, 083702 (2007).
86. Huang, B., Bates, M. & Zhuang, X. W. Super-resolution fluorescence microscopy. *Annu. Rev. Biochem.* **78**, 993–1016 (2009).
87. Hayden, J. H. & Allen, R. D. Detection of single microtubules in living cells - particle transport can occur in both directions along the same microtubule. *J. Cell Biol.* **99**, 1785–1793 (1984).
88. Schnapp, B. J., Vale, R. D., Sheetz, M. P. & Reese, T. S. Single microtubules from squid axoplams support bidirectional movement of organelles. *Cell* **40**, 455–462 (1985).
89. Burcik, E. & Plankenhorn, B. The demonstration of bacterial flagella by means of the phase microscope. *Arch. Mikrobiol.* **19**, 435–437 (1953).
90. Horio, T. & Hotani, H. Visualization of the dynamic instability of individual microtubules by dark-field microscopy. *Nature* **321**, 605–607 (1986).
91. Stemmer, A. Individual actin-filaments visualized by DIC (Nomarski) microscopy. *Biol. Bull.* **183**, 360–361 (1992).
92. Levene, M. J. *et al.* Zero-mode waveguides for single-molecule analysis at high concentrations. *Science* **299**, 682–686 (2003).
93. Woodside, M. T., García-García, C. & Block, S. M. Folding and unfolding single RNA molecules under tension. *Curr. Opin. Chem. Biol.* **12**, 640–646 (2008).
94. Chang, W. S., Ha, J. W., Slaughter, L. S. & Link, S. Plasmonic nanorod absorbers as orientation sensors. *Proc. Natl Acad. Sci. USA* **107**, 2781–2786 (2010).
95. Dunn, A. R. & Spudich, J. A. Dynamics of the unbound head during myosin V processive translocation. *Nature Struct. Mol. Biol.* **14**, 246–248 (2007).
96. Schultz, S., Smith, D. R., Mock, J. J. & Schultz, D. A. Single-target molecule detection with nonbleaching multicolor optical immunolabels. *Proc. Natl Acad. Sci. USA* **97**, 996–1001 (2000).
97. Axelrod, D., Thompson, N. L. & Burghardt, T. P. Total internal reflection fluorescent microscopy. *J. Microsc.* **129**, 19–28 (1983).
98. Molloy, J. E. & Veigel, C. Myosin motors walk the walk. *Science* **300**, 2045–2046 (2003).
99. Churchman, L. S., Okten, Z., Rock, R. S., Dawson, J. F. & Spudich, J. A. Single molecule high-resolution colocalization of Cy3 and Cy5 attached to macromolecules measures intramolecular distances through time. *Proc. Natl Acad. Sci. USA* **102**, 1419–1423 (2005).
100. Nishikawa, S. *et al.* Switch between large hand-over-hand and small inchworm-like steps in myosin VI. *Cell* **142**, 879–888 (2010).
101. Komori, Y., Iwane, A. H. & Yanagida, T. Myosin-V makes two brownian 90° rotations per 36-nm step. *Nature Struct. Mol. Biol.* **14**, 968–973 (2007).
102. Gordon, M. P., Ha, T. & Selvin, P. R. Single-molecule high-resolution imaging with photobleaching. *Proc. Natl Acad. Sci. USA* **101**, 6462–6465 (2004).
103. Qu, X. H., Wu, D., Mets, L. & Scherer, N. F. Nanometer-localized multiple single-molecule fluorescence microscopy. *Proc. Natl Acad. Sci. USA* **101**, 11298–11303 (2004).
104. Balci, H., Ha, T., Sweeney, H. L. & Selvin, P. R. Interhead distance measurements in myosin VI via SHRImP support a simplified hand-over-hand model. *Biophys. J.* **89**, 413–417 (2005).
105. Mori, T., Vale, R. D. & Tomishige, M. How kinesin waits between steps. *Nature* **450**, 750–754 (2007).
An important study that applied single-molecule FRET to analyse the relative position of the two heads of a kinesin motor during processive movement.
106. Sick, B., Hecht, B. & Novotny, L. Orientational imaging of single molecules by annular illumination. *Phys. Rev. Lett.* **85**, 4482–4485 (2000).
107. Toprak, E. *et al.* Defocused orientation and position imaging (DOPI) of myosin V. *Proc. Natl Acad. Sci. USA* **103**, 6495–6499 (2006).
108. Sosa, H., Peterman, E. J. G., Moerner, W. E. & Goldstein, L. S. B. ADP-induced rocking of the kinesin motor domain revealed by single-molecule fluorescence polarization microscopy. *Nature Struct. Biol.* **8**, 540–544 (2001).
109. Corrie, J. E. T. *et al.* Dynamic measurement of myosin light-chain-domain tilt and twist in muscle contraction. *Nature* **400**, 425–430 (1999).
110. Forkey, J. N., Quinlan, M. E., Shaw, M. A., Corrie, J. E. T. & Goldman, Y. E. Three-dimensional structural dynamics of myosin V by single-molecule fluorescence polarization. *Nature* **422**, 399–404 (2003).
111. Shiroguchi, K. & Kinosita, K. Myosin V walks by lever action and Brownian motion. *Science* **316**, 1208–1212 (2007).
112. Webb, M. R., Reid, G. P., Munasinghe, V. R. N. & Corrie, J. E. T. A series of related nucleotide analogues that aids optimization of fluorescence signals in probing the mechanism of P-loop ATPases, such as actomyosin. *Biochemistry* **43**, 14463–14471 (2004).
113. Ishijima, A. *et al.* Simultaneous observation of individual ATPase and mechanical events by a single myosin molecule during interaction with actin. *Cell* **92**, 161–171 (1998).
114. van Dijk, M. A., Kapitein, L. C., van Mameren, J., Schmidt, C. F. & Peterman, E. J. G. Combining optical trapping and single-molecule fluorescence spectroscopy: enhanced photobleaching of fluorophores. *J. Phys. Chem. B* **108**, 6479–6484 (2004).
115. Lang, M. J., Fordyce, P. M., Engh, A. M., Neuman, K. C. & Block, S. M. Simultaneous, coincident optical trapping and single-molecule fluorescence. *Nature Methods* **1**, 133–139 (2004).
116. Brau, R. R., Tarsa, P. B., Ferrer, J. M., Lee, P. & Lang, M. J. Interlaced optical force-fluorescence measurements for single molecule biophysics. *Biophys. J.* **91**, 1069–1077 (2006).
117. Boyer, D., Tamarat, P., Maali, A., Lounis, B. & Orrit, M. Photothermal imaging of nanometer-sized metal particles among scatterers. *Science* **297**, 1160–1163 (2002).
118. Mashanov, G. I. & Molloy, J. E. Automatic detection of single fluorophores in live cells. *Biophys. J.* **92**, 2199–2211 (2007).
119. Mortensen, K. I., Churchman, L. S., Spudich, J. A. & Flyvbjerg, H. Optimized localization analysis for single-molecule tracking and super-resolution microscopy. *Nature Methods* **7**, 377–381 (2010).
120. Helenius, J., Brouhard, G., Kalaidzidis, Y., Diez, S. & Howard, J. The depolymerizing kinesin MCAK uses lattice diffusion to rapidly target microtubule ends. *Nature* **441**, 115–119 (2006).

Describes a single-molecule fluorescence assay that showed that the microtubule-depolymerizing Kinesin-13 MCAK (mitotic centromere-associated kinesin; also known as KIF2C) uses 1D diffusion to reach the microtubule ends.

121. Okada, Y. & Hirokawa, N. A processive single-headed motor: kinesin superfamily protein KIF1A. *Science* **283**, 1152–1157 (1999).
122. Okada, Y. & Hirokawa, N. Mechanism of the single-headed processivity: diffusional anchoring between the K-loop of kinesin and the C terminus of tubulin. *Proc. Natl Acad. Sci. USA* **97**, 640–645 (2000).
123. Lu, H. L., Ali, M. Y., Bookwalter, C. S., Warshaw, D. M. & Trybus, K. M. Diffusive movement of processive Kinesin-1 on microtubules. *Traffic* **10**, 1429–1438 (2009).
124. Ali, M. Y. *et al.* Myosin Va maneuvers through actin intersections and diffuses along microtubules. *Proc. Natl Acad. Sci. USA* **104**, 4332–4336 (2007).
125. Ali, M. Y., Lu, H. L., Bookwalter, C. S., Warshaw, D. M. & Trybus, K. M. Myosin V and kinesin act as tethers to enhance each others' processivity. *Proc. Natl Acad. Sci. USA* **105**, 4691–4696 (2008).
126. Varga, V., Leduc, C., Bormuth, V., Diez, S. & Howard, J. Kinesin-8 motors act cooperatively to mediate length-dependent microtubule depolymerization. *Cell* **138**, 1174–1183 (2009).
127. Kapitein, L. C. *et al.* Microtubule-driven multimerization recruits ase1p onto overlapping microtubules. *Curr. Biol.* **18**, 1713–1717 (2008).
128. Kapitein, L. C. *et al.* The bipolar mitotic kinesin Eg5 moves on both microtubules that it crosslinks. *Nature* **435**, 114–118 (2005).
129. van den Wildenberg, S. *et al.* The homotetrameric Kinesin-5 KLP61F preferentially crosslinks microtubules into antiparallel orientations. *Curr. Biol.* **18**, 1860–1864 (2008).
130. Kwok, B. H. *et al.* Allosteric inhibition of Kinesin-5 modulates its processive directional motility. *Nature Chem. Biol.* **2**, 480–485 (2006).
131. Lakämper, S. *et al.* The effect of monastrol on the processive motility of a dimeric Kinesin-5 head/Kinesin-1 stalk chimera. *J. Mol. Biol.* **399**, 1–8 (2010).
132. Kapitein, L. C. *et al.* Microtubule cross-linking triggers the directional motility of Kinesin-5. *J. Cell Biol.* **182**, 421–428 (2008).
Single-molecule fluorescence was used here to observe the cargo-dependent switching on and off of a bipolar mitotic kinesin motor.
133. Harms, G. S., Cognet, L., Lommerse, P. H. M., Blab, G. A. & Schmidt, T. Autofluorescent proteins in single-molecule research: applications to live cell imaging microscopy. *Biophys. J.* **80**, 2396–2408 (2001).
134. Sako, Y. & Yanagida, T. Single-molecule visualization in cell biology. *Nature Rev. Mol. Cell Biol.* **4**, SS1–SS5 (2003).
135. Mashanov, G. I., Tacon, D., Peckham, M. & Molloy, J. E. The spatial and temporal dynamics of pleckstrin homology domain binding at the plasma membrane measured by imaging single molecules in live mouse myoblasts. *J. Biol. Chem.* **279**, 15274–15280 (2004).
136. Kural, C. *et al.* Kinesin and dynein move a peroxisome *in vivo*: a tug-of-war or coordinated movement? *Science* **308**, 1469–1472 (2005).
137. Nan, X. L., Sims, P. A., Chen, P. & Xie, X. S. Observation of individual microtubule motor steps in living cells with endocytosed quantum dots. *J. Phys. Chem. B* **109**, 24220–24224 (2005).
138. Leduc, C., Ruhnow, F., Howard, J. & Diez, S. Detection of fractional steps in cargo movement by the collective operation of Kinesin-1 motors. *Proc. Natl Acad. Sci. USA* **104**, 10847–10852 (2007).
139. Pierobon, P. *et al.* Velocity, processivity, and individual steps of single myosin V molecules in live cells. *Biophys. J.* **96**, 4268–4275 (2009).
140. Nelson, S. R., Ali, M. Y., Trybus, K. M. & Warshaw, D. M. Random walk of processive, quantum dot-labeled myosin Va molecules within the actin cortex of COS-7 Cells. *Biophys. J.* **97**, 509–518 (2009).
References 139 and 140 are landmark papers reporting the single-molecule observation of quantum-dot-labelled myosin V in cells.
141. Cai, D. W., Verhey, K. J. & Meyhofer, E. Tracking single kinesin molecules in the cytoplasm of mammalian cells. *Biophys. J.* **92**, 4137–4144 (2007).
142. Svoboda, K. & Block, S. M. Biological applications of optical forces. *Annu. Rev. Biophys. Biomol. Struct.* **23**, 247–285 (1994).
143. Knight, A. E., Veigel, C., Chambers, C. & Molloy, J. E. Analysis of single-molecule mechanical recordings: application to acto-myosin interactions. *Prog. Biophys. Mol. Biol.* **77**, 45–72 (2001).
144. Molloy, J. E. & Padgett, M. J. Lights, action: optical tweezers. *Contemp. Phys.* **43**, 241–258 (2002).
145. Simmons, R. M., Finer, J. T., Chu, S. & Spudich, J. A. Quantitative measurements of force and displacement using an optical trap. *Biophys. J.* **70**, 1813–1822 (1996).
146. Dupuis, D. E., Guilford, W. H., Wu, J. & Warshaw, D. M. Actin filament mechanics in the laser trap. *J. Muscle Res. Cell Motil.* **18**, 17–30 (1997).
147. Mehta, A. D., Finer, J. T. & Spudich, J. A. Detection of single-molecule interactions using correlated thermal diffusion. *Proc. Natl Acad. Sci. USA* **94**, 7927–7931 (1997).
148. van Mameren, J., Vermeulen, K. C., Gittes, F. & Schmidt, C. F. Leveraging single protein polymers to measure flexural rigidity. *J. Phys. Chem. B* **113**, 3837–3844 (2009).
149. Veigel, C., Bartoo, M. L., White, D. C. S., Sparrow, J. C. & Molloy, J. E. The stiffness of rabbit skeletal actomyosin cross-bridges determined with an optical tweezers transducer. *Biophys. J.* **75**, 1424–1438 (1998).
150. Steffen, W., Smith, D., Simmons, R. & Sleep, J. Mapping the actin filament with myosin. *Proc. Natl Acad. Sci. USA* **98**, 14949–14954 (2001).
151. Takagi, Y., Homsher, E. E., Goldman, Y. E. & Shuman, H. Force generation in single conventional actomyosin complexes under high dynamic load. *Biophys. J.* **90**, 1295–1307 (2006).
152. Visscher, K., Brakenhoff, G. J. & Krol, J. J. Micromanipulation by multiple optical traps created by a single fast scanning trap integrated with the bilateral confocal scanning laser microscope. *Cytometry* **14**, 105–114 (1993).
153. Valentine, M. T. *et al.* Precision steering of an optical trap by electro-optic deflection. *Opt. Lett.* **33**, 599–601 (2008).
154. Visscher, K., Schnitzer, M. J. & Block, S. M. Single kinesin molecules studied with a molecular force clamp. *Nature* **400**, 184–189 (1999).
The application of a single-molecule force clamp in an optical trap assay made it possible for these authors to study the force-dependence of the kinesin cycle with unprecedented accuracy.
155. Valentine, M. T., Fordyce, P. M., Krzysiak, T. C., Gilbert, S. P. & Block, S. M. Individual dimers of the mitotic kinesin motor Eg5 step processively and support substantial loads *in vitro*. *Nature Cell Biol.* **8**, 470–476 (2006).
156. Block, S. M., Asbury, C. L., Shaevitz, J. W. & Lang, M. J. Probing the kinesin reaction cycle with a 2D optical force clamp. *Proc. Natl Acad. Sci. USA* **100**, 2351–2356 (2003).
157. Rief, M. *et al.* Myosin-V stepping kinetics: a molecular model for processivity. *Proc. Natl Acad. Sci. USA* **97**, 9482–9486 (2000).
158. Wang, M. D. *et al.* Force and velocity measured for single molecules of RNA polymerase. *Science* **282**, 902–907 (1998).
159. Greenleaf, W. J., Woodside, M. T., Abbondanzieri, E. A. & Block, S. M. Passive all-optical force clamp for high-resolution laser trapping. *Phys. Rev. Lett.* **95**, 208102 (2005).
160. Abbondanzieri, E. A., Greenleaf, W. J., Shaevitz, J. W., Landick, R. & Block, S. M. Direct observation of base-pair stepping by RNA polymerase. *Nature* **438**, 460–465 (2005).
161. Greenleaf, W. J., Frieda, K. L., Foster, D. A. N., Woodside, M. T. & Block, S. M. Direct observation of hierarchical folding in single riboswitch aptamers. *Science* **319**, 630–633 (2008).
162. Woodside, M. T. *et al.* Direct measurement of the full, sequence-dependent folding landscape of a nucleic acid. *Science* **314**, 1001–1004 (2006).
163. Gittes, F. & Schmidt, C. F. Thermal noise limitations on micromechanical experiments. *Eur. Biophys. J.* **27**, 75–81 (1998).
164. Gittes, F. & Schmidt, C. F. in *Methods in Cell Biology*, Vol. 55 (*Laser Tweezers in Cell Biology*) (Ed. M. P. Sheetz) 129–156 (Academic Press Inc., San Diego, 1998).
A basic introduction to the analysis of single-molecule optical-trap data and a discussion of relevant noise sources.
165. Smith, D. A., Steffen, W., Simmons, R. M. & Sleep, J. Hidden-Markov methods for the analysis of single-molecule actomyosin displacement data: the variance-Hidden-Markov method. *Biophys. J.* **81**, 2795–2816 (2001).
166. Capitanio, M. *et al.* Two independent mechanical events in the interaction cycle of skeletal muscle myosin with actin. *Proc. Natl Acad. Sci. USA* **103**, 87–92 (2006).
167. Lewalle, A., Steffen, W., Stevenson, O., Ouyang, Z. Q. & Sleep, J. Single-molecule measurement of the stiffness of the rigor myosin head. *Biophys. J.* **94**, 2160–2169 (2008).
168. Lister, I. *et al.* A monomeric myosin VI with a large working stroke. *EMBO J.* **23**, 1729–1738 (2004).
169. Laakso, J. M., Lewis, J. H., Shuman, H. & Ostap, E. M. Myosin I can act as a molecular force sensor. *Science* **321**, 133–136 (2008).
170. Gebhardt, J. C. M., Okten, Z. & Rief, M. The lever arm effects a mechanical asymmetry of the myosin-V–actin bond. *Biophys. J.* **98**, 277–281 (2010).
171. Oguchi, Y. *et al.* Robust processivity of myosin V under off-axis loads. *Nature Chem. Biol.* **6**, 300–305 (2010).
172. Uemura, S. & Ishiwata, S. Loading direction regulates the affinity of ADP for kinesin. *Nature Struct. Biol.* **10**, 308–311 (2003).
173. Ashkin, A., Schutze, K., Dziedzic, J. M., Euteneuer, U. & Schliwa, M. Force generation of organelle transport measured *in vivo* by an infrared laser trap. *Nature* **348**, 346–348 (1990).
174. Welte, M. A., Gross, S. P., Postner, M., Block, S. M. & Wieschaus, E. F. Developmental regulation of vesicle transport in *Drosophila* embryos: forces and kinetics. *Cell* **92**, 547–557 (1998).
175. Shubeita, G. T. *et al.* Consequences of motor copy number on the intracellular transport of Kinesin-1-driven lipid droplets. *Cell* **135**, 1098–1107 (2008).
176. Agayan, R. R., Gittes, F., Kopelman, R. & Schmidt, C. F. Optical trapping near resonance absorption. *Appl. Opt.* **41**, 2318–2327 (2002).
177. Laib, J. A., Marin, J. A., Bloodgood, R. A. & Guilford, W. H. The reciprocal coordination and mechanics of molecular motors in living cells. *Proc. Natl Acad. Sci. USA* **106**, 3190–3195 (2009).
178. Mizuno, D., Bacabac, R., Tardin, C., Head, D. & Schmidt, C. F. High-resolution probing of cellular force transmission. *Phys. Rev. Lett.* **102**, 168102 (2009).
179. Mizuno, D., Tardin, C., Schmidt, C. F. & MacKintosh, F. C. Nonequilibrium mechanics of active cytoskeletal networks. *Science* **315**, 370–373 (2007).
180. Bobroff, N. Position measurement with a resolution and noise-limited instrument. *Rev. Sci. Instr.* **57**, 1152–1157 (1986).
181. Thompson, R. E., Larson, D. R. & Webb, W. W. Precise nanometer localization analysis for individual fluorescent probes. *Biophys. J.* **82**, 2775–2783 (2002).
A fundamental discussion of attainable accuracy in localizing single fluorescent molecules in a microscope.
182. Dillingham, M. S. & Wallace, M. I. Protein modification for single molecule fluorescence microscopy. *Org. Biomol. Chem.* **6**, 3031–3037 (2008).
183. Fu, C. C. *et al.* Characterization and application of single fluorescent nanodiamonds as cellular biomarkers. *Proc. Natl Acad. Sci. USA* **104**, 727–732 (2007).
184. Tisler, J. *et al.* Fluorescence and spin properties of defects in single digit nanodiamonds. *ACS Nano* **3**, 1959–1965 (2009).
185. Bachilo, S. M. *et al.* Structure-assigned optical spectra of single-walled carbon nanotubes. *Science* **298**, 2361–2366 (2002).
186. Vale, R. D. & Milligan, R. A. The way things move: looking under the hood of molecular motor proteins. *Science* **288**, 88–95 (2000).
187. Ando, T. *et al.* High-speed atomic force microscopy for capturing dynamic behavior of protein molecules at work. *e-J. Surf. Sci. Nanotech.* **3**, 384–392 (2005).

Acknowledgments
We thank the Medical Research Council, UK (C.V.) and the Deutsche Forschungsgemeinschaft (Center for Molecular Physiology of the Brain, (CMPB)) (C.F.S.) for financial support.

Competing interests statement
The authors declare no competing financial interests.

FURTHER INFORMATION
Claudia Veigel's homepage:
http://www.cell.physiol.med.uni-muenchen.de/index.html
Christoph F. Schmidt's homepage:
http://www.dpi.physik.uni-goettingen.de/en/forschung/prof-schmidt.html

ALL LINKS ARE ACTIVE IN THE ONLINE PDF